

**The association between peak resultant linear acceleration and brain tissue deformation in American football-related helmeted head impacts**

**Katrina Zanetti**

A thesis submitted to  
The Faculty of Graduate and Postdoctoral Studies of the University of Ottawa  
In partial fulfillment of the requirements for the degree for  
Master of Science in Human Kinetics

**Advisor**

Thomas B. Hoshizaki, PhD

**Committee Members**

Gordon Robertson, PhD

Heidi Sveistrup, PhD

Faculty of Health Sciences  
School of Human Kinetics

University of Ottawa

## Acknowledgements

I would like to thank all of the individuals who have helped me make this work possible. I would firstly like to acknowledge the assistance of my graduate studies supervisor, Dr. Blaine Hoshizaki. I consider it a true privilege to have worked with and learned from such a successful and world-known researcher in the field of head impact biomechanics. When I began as a Master's student, I couldn't have imagined how much I had ahead of me to learn. Thank you for all of the guidance and life advice as well that you have given me throughout the whole process. It has been invaluable. I would also like to thank Dr. Heidi Sveistrup and Dr. Gordon Robertson for sitting on my thesis committee, for all of their expertise in helping me complete this work. Thank you for giving me valuable feedback along each step of the process that helped my research become so much better.

I am also grateful for the tremendous love and support shown to me throughout this process from the people who are closest to me. I would like to thank my parents, Fabio and Lisa Zanetti, for your encouragement during this chapter of my life and for the amazing role models you both are to me. Thanks for teaching me that anything worth having in life takes extremely hard work. Mom, thanks for putting up with me when I was stressed out beyond belief. Dad, you are so much of a role model to me as someone who has worked very hard to get to where they are now. Thank you also to the love of my life Andrew Rollins, for the unconditional love and understanding you have shown me throughout this journey that have been nothing less than incredible. You inspire me to keep being better and to keep persevering. Thanks for always believing in me and for being my biggest fan, and for your commitment to putting up with two additional years of being long-distance. I am also grateful to my amazing friends who encouraged me throughout this whole endeavor and kept my spirits high when I needed it.

I would also like to thank my colleagues who have been by my side throughout my time as a graduate student: Andrew, Phil, Marshall, Anna, Clara, Evan, Karen, Janie, Dave, and everyone else. I feel so fortunate to have had the opportunity to work with such talented individuals and such a great, close-knit group of coworkers. Thank you for the advice, support, and all the encouragement to keep going.

I sincerely could not have done this research without every person mentioned here and others. I feel very blessed to have so many people in my life who have helped me complete this work and get to where I am now.

## Abstract

The objective of this study was to determine the degree of association of peak resultant linear acceleration with maximum principal strain, von Mises stress, and strain rate in the cerebrum. Three prevalent head impact mechanisms in the sport of football were represented by impacting an accelerometer-outfitted Hybrid III headform. Head to head impacts were characterized using a linear impactor, falls to the ground using a monorail drop, and elbow or forearm strikes to the head by a pendulum system. Representative inbound impact velocities were selected according to epidemiological research. Impacts were performed at nine prescribed centric and non-centric sites on the head. Finite element modeling using the University College Brain Trauma Model was employed to obtain peak values of maximum principal strain, von Mises stress, and strain rate in the cerebrum. Pearson product-moment correlation coefficients ( $r$ ) were calculated between peak resultant linear acceleration of the head and peak MPS, VMS, and strain rate in order to determine the degree of correlation between the variables. This was determined for each impact mechanism and location as well as for all mechanisms together. Significant correlations ( $p < 0.05$ ) between peak linear acceleration and the three metrics of tissue deformation were found for particular mechanisms of impact. For each of MPS, VMS, and strain rate, impacts conducted on the pendulum system, meant to replicate arm to head impacts, did not have a significant correlation with linear acceleration. In contrast, the head to head mechanism of impact resulted in significant correlation coefficients between linear acceleration and all metrics of tissue deformation. The strength of the correlation was not significantly different when centric versus non-centric impact sites were compared. Overall, characteristics of a head impact such as the inbound energy, whether the vector of impact was centric or non-centric, and the degree of energy transfer that occurs through the head upon impact, likely play a role in the resulting degree of correlation between linear acceleration and brain tissue deformation.

# Table of Contents

LIST OF TABLES	vii
LIST OF FIGURES	viii
LIST OF EQUATIONS	ix
<u>CHAPTER 1</u> <u>Introduction</u>	1
1.1 Statement of the Problem	2
1.2 Significance	4
1.3 Experimental research Hypotheses	5
1.4 Variables	6
1.5 Delimitations	6
1.6 Limitations	7
1.7 Objective	7
<u>CHAPTER 2</u> <u>Review of Literature</u>	9
2.1 Injury Mechanism	10
2.2 The Spectrum of Brain Injuries	11
2.3 Pathophysiology	13
2.4 Impact Mechanics	14
2.4.1 Peak linear acceleration	14
2.4.2 Peak rotational acceleration	15
2.4.3 Brain tissue deformation metrics	16
2.4.4 Thresholds of Injury	17
2.4.5 Kinematics and brain tissue deformation correlation	19
2.5 Finite Element Modeling	21
2.5.1 University College Dublin Brain Trauma Model	21

2.5.1.1 Model Development	21
2.5.1.2 Material Properties of the Model	22
2.5.1.3 Validation of the Model	25
2.5.1.4 Research using the University College Dublin Brain Trauma Model	26
2.6 Summary	26
<u>CHAPTER 3</u> <u>Methods</u>	28
3.1 Apparatus	28
3.1.1 Pneumatic linear impactor	28
3.1.2 Pendulum system	29
3.1.3 Monorail drop system	30
3.1.4 Hybrid III head- and neckform	31
3.1.5 Collection System	32
3.2 Description of Impact Conditions	33
3.2.1 Impact velocity	33
3.2.2 Impact location	34
3.2.3 Impact mechanism	34
3.3 Procedure	35
3.3.1 Head Impacts	35
3.3.2 Finite element analysis of brain trauma	36
3.5 Research Design	36
3.6 Statistical Analysis	38
<u>CHAPTER 4</u> <u>Results</u>	40
4.1 Correlation with maximum principal strain	44
4.2 Correlation with von Mises stress	50

4.3 Correlation with strain rate	56
<u>CHAPTER 5 Discussion</u>	63
5.1 Correlation of linear acceleration with brain tissue deformation metrics	63
5.2 Influence of impact location and mechanism on the relationship between linear acceleration and deformation metrics	68
5.3 Significance	71
<u>CHAPTER 6 Conclusions</u>	74
6.1 Research Hypotheses	74
6.2 Summary	75
References	77
Appendix A: Impact Locations: University of Ottawa Test Protocol-9	83

## LIST OF TABLES

Table 1. Finite element model material properties

Table 2. Summary of the three impact conditions

Table 3. Research design

Table 4. Peak resultant linear acceleration results in  $g$

Table 5. Maximum principal strain results

Table 6. Von Mises stress results in Pa

Table 7. Strain rate results in  $s^{-1}$

Table 8. Pearson correlations between linear acceleration and MPS by impact mechanism

Table 9. Pearson correlations between linear acceleration and MPS by impact location

Table 10. Pearson correlations between linear acceleration and VMS by impact mechanism

Table 11. Pearson correlations between linear acceleration and VMS by impact location

Table 12. Pearson correlations between linear acceleration and strain rate by impact mechanism

Table 13. Pearson correlations between linear acceleration and strain rate by impact location

## LIST OF FIGURES

Figure 1. Linear impactor prior to pneumatic release; unhelmeted Hybrid III head- and neckform immediately prior to striker contact

Figure 2. Pendulum frame, circular metal plates, and MEP impactor cap

Figure 3. Unhelmeted Hybrid III head and neckform attached to monorail drop rig and impacting a MEP anvil

Figure 4. Hybrid III head- and neckform mounted on sliding table

Figure 5. Scatterplot of Peak Linear Acceleration versus MPS for head to head impact mechanism

Figure 6. Scatterplot of Peak Linear Acceleration versus MPS for arm to head impact mechanism

Figure 7. Scatterplot of Peak Linear Acceleration versus MPS for fall impact mechanism

Figure 8. Scatterplot of Peak Linear Acceleration versus MPS for all impact mechanisms

Figure 9. Scatterplot of Peak Linear Acceleration versus VMS for head to head impact mechanism

Figure 10. Scatterplot of Peak Linear Acceleration versus VMS for arm to head impact mechanism

Figure 11. Scatterplot of Peak Linear Acceleration versus VMS for fall impact mechanism

Figure 12. Scatterplot of Peak Linear Acceleration versus VMS for all impact mechanisms

Figure 13. Scatterplot of Peak Linear Acceleration versus Strain rate for head to head impact mechanism

Figure 14. Scatterplot of Peak Linear Acceleration versus Strain rate for arm to head impact mechanism

Figure 15. Scatterplot of Peak Linear Acceleration versus Strain rate for fall impact mechanism

Figure 16. Scatterplot of Peak Linear Acceleration versus Strain rate for all impact mechanisms

## LIST OF EQUATIONS

Equation 1: Hyperelastic Law

$$C_{10}(t) = 0.9C_{01}(t) = 620.5 + 1930e^{-t/0.008} + 1103e^{-t/0.15} \text{ (Pa)}$$

Where  $C_{10}$  and  $C_{01}$  are the temperature-dependent material parameters, and  $t$  is time in seconds.

Equation 2: Shear characteristics of the viscoelastic behaviour of the brain

$$G(t) = G_{\infty} + (G_0 - G_{\infty})e^{-\beta t}$$

Where  $G_{\infty}$  is the long term shear modulus,  $G_0$  is the short term shear modulus and  $\beta$  is the decay factor.

Equation 3: Headform angular acceleration component (x)

$$\vec{\alpha}_x = \frac{a_{zS} - a_{zC}}{2S} - \frac{a_{yT} - a_{yC}}{2T}$$

Equation 4: Headform angular acceleration component (y)

$$\vec{\alpha}_y = \frac{a_{xT} - a_{xC}}{2T} - \frac{a_{zF} - a_{zC}}{2F}$$

Equation 5: Headform angular acceleration component (z)

$$\vec{\alpha}_z = \frac{a_{yF} - a_{yC}}{2F} - \frac{a_{xS} - a_{xC}}{2S}$$

Where  $\alpha_i$  is the angular acceleration for component  $i$  (x, y, z),  $a_{ij}$  is the linear acceleration for component  $i$  (x, y, z) along orthogonal arm  $j$  (frontal, sagittal, transverse).

# CHAPTER 1

## Introduction

Mild traumatic brain injuries (mTBIs) have become a major health concern worldwide; the Center for Disease Control and Prevention in the United States has estimated that as many as 300,000 mTBIs occur as a result of sport each year (Centers for Disease Control and Prevention, 1997). Concussions, or mTBIs, are common occurrences even when players wear protective headgear in both recreational and professional sports (Delaney et al., 2002). Recent research supports an association between impact exposure and recurrent concussions contributing to long-term and chronic neurological consequences. Neurodegenerative disease associated with repetitive brain trauma has been associated with playing American football specifically (Harmon et al., 2013). Research investigating one such condition, chronic traumatic encephalopathy (CTE), has noted that repetitive head trauma is necessary for development of the disease. However, it is likely not sufficient, as only a subset of the brains of sports players with high levels of brain trauma show signs of CTE post-mortem (Baugh et al., 2012). In addition to the health-related burden imposed by head injuries, they introduce a significant economic burden on the healthcare system. A study examining head injuries that resulted in hospitalization reported a direct medical cost for one individual of approximately \$20,000 – 29,000 [in 2011 USD], and indirect costs to be as high as \$700,000 over a lifetime

[2011 USD]. Indirect costs result from the loss of productivity attributed to a victim's absence from the workforce and their decreased productivity (Max et al., 1991).

In this thesis, the relationship between peak resultant linear acceleration of the head and subsequent brain tissue deformation was investigated. Exploring this relationship is important because peak linear acceleration is widely used as the principal measure of brain trauma, particularly concussion. It is the main metric of head impact severity used by developers of certification standards for helmets and impact count devices that are intended to reflect brain trauma, particularly concussion. Currently however, the quantitative association between linear acceleration and brain tissue deformation remains unknown. It is important to investigate because knowledge of brain injury risk for football players based on the impacts they sustain will help to develop effective preventive strategies unique to the particular hit types these players encounter.

### **1.1 Statement of the Problem**

Of all concussions that occur secondary to sport in the United States each year, American football is responsible for the largest incidence of any sport (Thunman et al., 1998). Although estimates vary due to population sample and injury criteria used, research has reported that as many as 19% of American football players have experienced a mild traumatic brain injury (Guskiewicz et al., 2000; Covassin et al., 2003). A multiyear investigation of concussion in professional football by Pellman et al. (2004) reports a concussion incidence of  $131.2 \pm 26.8$  per year, at an average rate of 0.41 concussions per National Football League game. Due to the stigma associated with concussions being inconsequential injuries, research

has shown that the proportion of football players having experienced mild traumatic brain injury (mTBI) symptoms in the past increased to 47% when the word “concussion” was removed from a questionnaire asking about experiencing concussion symptoms (Langburt et al., 2001). Similarly, approximately 45% of Canadian Football League players and 70% of inter-university football players in Canada reported experiencing mTBI-related symptoms (Delaney et al., 2000; 2002). This research suggests that concussions are often under-reported in sport settings, which is not unlike the underestimation of the true prevalence of concussion that has been reported for mTBIs in the general population (Leibson et al., 2012). It is estimated that almost half (47%) of concussions in high school football go unreported (McCrea et al., 2004).

Risks associated with sustaining an mTBI unique to football remain largely elusive considering the significant amount of epidemiological research that has been done. Crisco and colleagues (2011) used the head impact telemetry (HIT) system to study collegiate players over three years and reported that frequencies of head impacts varied considerably by both impact location on the helmet and player position. They found that the highest magnitude impacts were sustained by running backs and quarter backs, while offensive and defensive linemen and linebackers experienced head impacts at a frequency almost twice that of any other position (Guskiewicz et al., 2005). Reconstruction research of National Football League (NFL) plays mirrors these estimations; after adjustment of injury rates for the number of players in each position group, the relative risk of concussion was also reported to be highest for quarterbacks (1.62 concussions per 100 game-positions) (Pellman et al., 2004). Although some players positions in football may experience impacts of lesser magnitude, research suggests that repetitive impacts may be associated with chronic brain injury. A link has been reported

between retired professional football players who sustained recurrent concussions and subsequent development of memory-related symptoms (Guskiewicz et al., 2005). Sub-concussive head injury with adequate linear acceleration to result in a non-structural injury, which fails to present with typical clinical symptoms but does result in neuronal changes, is suspected to be sufficient to initiate the neurodegenerative cascade (Baugh et al., 2012). Chronic traumatic encephalopathy (CTE), a progressive tauopathy, has been shown to exist in increasingly severe states according to both the degree of neuropathology present and symptom presentation (McKee et al., 2013). However, identifying the cause of CTE as repeated concussive or sub-concussive impacts has not been successful. There is a correlation between the two; the presentation of athletes with CTE may reflect intrinsic inter-individual differences rather than the syndrome being caused by repetitive head trauma alone. Further epidemiological research is needed to establish a repetitive trauma cause of CTE with certainty (McCrory et al., 2013). Overall, there is ample evidence that football is associated with a high risk of head injury and as a result, efforts are needed to increase head protection for this sport.

## **1.2 Significance**

In order to decrease risk of concussion, understanding the biomechanical underpinnings of these injuries and the resulting trauma to the brain is critical. Impacts to the head are influenced by a variety of factors including location on the head, mass, velocity, angle, and compliance of the impacting object. A better understanding of neurological risks associated with hits to the head in football requires knowledge of the most effective metrics for reflecting trauma to the brain. For the most part, head trauma in sport is reported as peak

resultant acceleration. Measuring peak rotational acceleration is challenging, as particular accelerometers and equipment is needed. In contrast, peak resultant linear acceleration can be determined with relatively less difficulty. So, it is important to investigate the accuracy with which linear acceleration captures the degree of brain tissue deformation and trauma.

The information obtained from this research will provide knowledge about descriptors of brain trauma; specifically, the effectiveness of peak resultant head linear acceleration as a measure for brain trauma. It is hoped that this knowledge will support the understanding of the relationship between peak linear acceleration and the risk of neurological symptoms and complications caused by trauma to the brain. In the future the degree of head injury risk could be known, predicted, and managed before clinical signs appear.

An additional application of this study's findings relates to the effectiveness of head impact sensor technology. Such impact sensors are beginning to be developed by manufacturers and are intended to alert players of various sports of potentially damaging head impacts. In turn, knowing the effectiveness with which linear acceleration represents brain tissue deformation will also provide valuable information for the development of protective equipment. In particular, this study's findings will be useful for improving the way impact sensors and counters measure the trauma to the brain during sporting events.

### **1.3 Experimental Research Hypotheses**

H1: Peak resultant linear acceleration (PLA) and maximum principal strain (MPS) will have low positive correlation ( $r < 0.5$ ) for all impact mechanisms and locations.

H2: PLA and von Mises stress (VMS) will have low positive correlation ( $r < 0.5$ ) for all impact mechanisms and locations.

H3: PLA and strain rate will have low positive correlation ( $r < 0.5$ ) for all impact mechanisms and locations.

## **1.4 Variables**

### *1.4.1 Independent variables*

1. Impact mechanism (3 levels: head to head; forearm or elbow to head; head to ground);
2. Impact location (9 levels: according to UOTP<sup>9</sup> protocol) (See Appendix A).

### *1.4.2 Dependent variables*

1. Peak resultant linear acceleration ( $g$ );
2. Maximum principal strain;
2. von Mises stress;
3. Strain rate.

## **1.5 Delimitations**

Only three impact mechanisms at three velocities and nine locations on the head were tested three times each, for a total of 81 impacts. It is understood that the relationship between resultant peak linear acceleration and brain tissue deformation (as measured by MPS, VMS, and strain rate) may deviate from the results of this study for impact mechanisms, velocities, or locations that were not specifically tested. As a result, the degree of correlation

between these two metrics determined by this research cannot necessarily be widely applied to impacts typically experienced by football players in every playing position and of all skill levels.

## **1.6 Limitations**

Three brain tissue deformation metrics were used in this study to describe brain trauma. These variables are measures of deformation; however the strength of the relationship between tissue deformation and linear acceleration is important in interpreting the peak linear acceleration data.

The 50<sup>th</sup> percentile adult male Hybrid III headform was used as a human surrogate in this research. The Hybrid III is the most commonly used head dummy, but it is not fully biofidelic and does not provide exact perfect dynamic response characteristics of the head (Deng 1989; Seemann, Muzzy & Lustick, 1986). However, the Hybrid III headform is the standard anthropomorphic head dummy used in the industry due to its ability to tolerate high-force and high-velocity impacts. Although efforts were made to ensure that the headform was outfitted with a standard football helmet worn by players in the event, the actual trauma experienced by the player may have differed from what was calculated in this study due to varying attenuation characteristics of the different helmet models.

## **1.7 Objective**

The aim of this research was to determine the degree of association of peak resultant linear acceleration with brain tissue deformation metrics in football-related head impacts.

Peak resultant linear acceleration and brain tissue deformation, as quantified by modeled stress and strain variables, were measured for a variety of conditions representative of head impacts commonly encountered in football. The degree to which the two measures correlate provided information about the accuracy of linear acceleration-based head protection strategies during football.

Determining the degree of correlation between peak resultant linear acceleration of the head and brain tissue deformation was accomplished by impacting a helmeted Hybrid III headform according to three mechanisms of impact typical of football. For each mechanism, nine distinct locations on the headform were tested. Inbound velocity of each of the three mechanisms reflected realistic levels for each mechanism. Stratifying impact conditions by mechanism and location on the head provided a range of tissue deformation variables. This defined the relationship between linear acceleration and brain tissue deformation across potential injury mechanisms. Comparing linear acceleration and MPS, VMS, and strain rate for a variety of impact locations on the head demonstrated whether the same association between the two parameters exists for centric and non-centric impacts.

## CHAPTER 2

### Review of Literature

Recent research comparing twenty different sports reported football as responsible for the highest injury rate among high school athletes (47%). The next highest incidence was reported for girls' soccer which was responsible for only 8% of sport-related concussions (Marar et al., 2012). Across all age groups, the true prevalence of mTBI in the population is likely greater as this quantity is believed to be an underestimation: many milder cases go unreported and undocumented in the health care system (Leibson et al., 2012). Brain injury was the cause of 69% of fatalities in American football players during the years 1945 to 1999 (Cantu & Mueller 2003). However, throughout the history of American football as a sport, catastrophic injuries have dramatically decreased with the advent of certified helmet use (Levy et al., 2004).

This chapter will discuss the injury mechanism and velocity of impact, particularly in the game of American football, the continuum along which brain injuries can present, and known predictors. The types of impacts according to mechanism typically observed in this sport, as well as the frequency that each is encountered, will also be presented. A brief background on brain tissue deformation metrics and finite element modeling of the brain will follow.

## 2.1 Injury Mechanism

The mechanism of injury was used to describe the mechanical input associated with brain tissue deformation. as Brain contusions have been described as resulting from movement of the brain within the skull and skull deformation; impacts result from intracranial pressure gradients; the skull and brain undergo motion relative to one another due to rotation of the head. Real-world head impacts result in a combination of linear and rotational acceleration of the head (Post & Hoshizaki, 2012).

While a head injury in football can occur via a variety of mechanisms., the majority (67.7%) of concussive impacts result from an impact by another helmet, followed by striking other body parts (20.9%) and contact with the ground (11.4%) (Pellman et al., 2004).

Impact velocities for head to head impacts in football have been reported between 3.1 - 11.7 m/s (Pellman et al., 2003). Withnall and colleagues (2005) measured head accelerations upon impact by another player's head and upper extremity during football reporting head impacts with upper extremities as occurring 38% of the time, by another player's helmet as occurring 30% of the time, with the remainder of hits attributed to the knee, football, and foot. These researchers reported a range of velocities of the impacting body part for elbow to head impacts as 1.7 to 4.6 m/s. Similarly the hand, wrist, or forearm was reported to strike the head at a velocity of 5.2 to 9.3 m/s (Withnall et al., 2005). These laboratory simulations were not reconstructions of diagnosed concussions, however the authors linked various impact mechanisms to risk of concussion. Hits to the head by the hand, wrist, or forearm were associated with a low risk of concussion (< 5%). However, re-enactments of head to head

impacts in football resulted in high concussion risk (as high as 67%) in this study (Withnall et al., 2005).

Regardless of striking object, the head is subjected to forces when contact occurs, resulting in linear and rotational accelerations. The first of these two types of motion, linear or translational acceleration, is the outcome of the total applied force passing directly through the head's centre of gravity. Rotational, or angular, acceleration is produced by the moment of a force about the centre of gravity of the head and results in rotation of the head. In real-world head injuries, both types of motion of the head are simultaneously present at variable levels (Ommaya, Goldsmith, & Thibault, 2002).

## **2.2 The Spectrum of Brain Injuries**

A brain injury can range from mild concussion to severe traumatic injuries including brain contusions, subdural hematomas, and intracranial bleeds. According to the American Association of Neurological Surgeons, a concussion, at the mild end of the injury spectrum, is described as “a clinical syndrome characterized by immediate and transient alteration in brain function, including alteration of mental status and level of consciousness, resulting from mechanical force or trauma” (2011). Symptoms are widely variable between individuals, or may be absent altogether, making definitive diagnosis of concussion difficult.

Traumatic injuries comprise the more severe end of the brain injury spectrum. A contusion is diagnosed when the brain tissue becomes bruised as a result of the impact and involves bleeding and swelling of the brain. Contusions often occur in cases in which the brain comes into contact with the skull and severity is directly correlated with the degree of energy

transferred at time of impact (Nolan 2005). A hematoma is a blood clot that collects around the brain and can cause increasing pressure within the restriction of the skull (American Association of Neurological Surgeons 2011). Hematomas can be either subdural (bleeding below the dura mater; between the dura and arachnoid layers) or epidural (above the dura mater; between the dura and skull). Cerebral edema can occur in the surrounding tissues of the brain, which can subsequently lead to increased intracranial pressure (ICP). This increase in ICP can also present harmful secondary effects such as ischemia (Nolan 2005).

Post concussive syndrome (PCS) is a condition in which symptoms of a mild TBI persist beyond the normal span of time for symptom resolution and has an assortment of negative cognitive, emotional, and memory effects associated with it. The nature and severity of impacts that cause PCS, if distinct at all from concussive impacts, are currently elusive. However, research comparing the linear and rotational acceleration of reconstructed injuries that resulted in PCS showed that the linear acceleration of these cases was of a comparable magnitude to concussion cases. However, the rotational acceleration of the PCS cases was not significantly different from the rotational acceleration of TBI cases. This suggests a potentially distinct mechanism of injury for PCS cases from concussion. It demonstrates that linear acceleration alone does not always reflect the degree of brain trauma; it may be insufficient, without considering rotational acceleration, to discriminate between impacts of various severities along the brain injury spectrum (Oeur et al., 2013).

The Glasgow Coma Scale is one tool commonly used to characterize the degree of severity of a brain injury sustained by a patient. It is based on three categories of commonly seen impairments: motor responsiveness, verbal performance, and eye opening to an

appropriate stimulus. A numerical score is given to a patient for each of these three categories, and the combined score allows for quick classification of the severity of injury. The associated classifications are as follows: severe TBI is indicated by a score of  $\leq 8$ ; a score between 9 and 12 indicates moderate TBI; mild TBI is indicated by 13 – 15 (American College of Surgeons, 1998).

### **2.3 Pathophysiology**

Among National Football League (NFL) players, the incidence of “nervous system” related deaths has recently been increasing; in particular, several players were documented to have retired due to unresolved neurological issues which may be associated with recurrent mTBIs (Pellman, 2003). An epidemiological study on the neurodegenerative causes of death among retired NFL players showed that standardized mortality ratios for “speed” playing positions (quarterback, running back, halfback, fullback, wide receiver, tight end, defensive back, safety, and linebacker) were three times higher for all neurodegenerative causes combined, compared to the overall male population in the United States. Long term repeated trauma to the head including the sequelae of concussion, especially repeated concussions, is associated with serious clinical conditions. The link between biomechanical profiles of trauma to the brain and these resulting clinical outcomes has yet to be described in the literature.

Research investigating potential biomarkers of minor central nervous system injuries in Olympic boxers found that elevated cerebrospinal fluid (CSF) levels of T-tau, NFL, GFAP, and S-100B were found in 80% of the boxers post head trauma. Interestingly, these changes were observed even in the absence of typical clinical symptoms of concussion. The time before the

athlete has recovered from an acute injury is suggested to serve as a critical period, during which additional injury can have serious and cumulative effects. In many of the boxers, neurofilament light protein (NFL) and glial fibrillary acidic protein (GFAP) failed to return to normal levels, which the study's authors suggested could be indicative of long-term neural tissue degeneration (Neselius et al., 2012). This research provides evidence for a biochemical and physiological outcome of the mechanical nature of head impacts in boxing. Similar biomarker alteration may occur in football players who have sustained multiple mTBIs as well.

To date, uncertainty surrounds the lower-bound threshold describing the minimum level of head trauma to be formally considered an injury. The lowest level of physical trauma necessary to result in neurological changes, which are mirrored in changes in biomarker levels, has yet to be defined. In addition, the most effective metric that quantifies this minimum threshold has yet to be determined. This study's objective of examining the correlation of peak linear acceleration with metrics of brain deformation addresses the question of the ability of linear acceleration as a metric of minimum trauma to result in clinical injury.

## **2.4 Impact Mechanics**

### *2.4.1 Peak linear acceleration*

Although research has shown that brain strain or deformation is the principal cause of injury, measurement of these values *in vivo* is not feasible. Thus, other metrics such as acceleration of the head upon impact must be used as proxies for determining the injury mechanism (King et al., 2003). Linear acceleration has been linked to focal brain injuries (King et al., 2003) and skull deformation and intracranial pressure alterations, both of which are

associated with brain trauma (Gurdjian & Lissner, 1944; Gurdjian et al., 1953). Changes in intracranial pressure are believed to be a potential injury mechanism as they can result in harmful shear stresses to brain tissue. Pressure changes occur because of skull deformation and acceleration post-impact, which is one way in which risk of injury is predicted. Peak linear acceleration has been the primary variable used to measure the risk for concussion (Gurdjian et al., 1955). However, recent real life injury reconstructions have demonstrated horizontal translation of the head produced focal effects responsible for contusions and cerebral hematomas, but rotational acceleration during an impact was required for diffuse injury as described by Gennarelli and coworkers (1971, 1972).

Recent analyses of reconstructions of professional football impacts revealed that high peak linear acceleration of the head was the principal correlate with concussion outcome, even more than its rotational acceleration (Pellman et al., 2003). Although peak linear acceleration is used as a metric for impact severity and injury, its relationship with variables of brain tissue deformation has not been quantified.

#### *2.4.2 Peak rotational acceleration*

Holbourn (1943) identified head rotational acceleration as a key head injury mechanism, it was suggested that this movement of the head could generate shear strain and tensile strain which was hypothesized to contribute to cerebral concussion. Experiments using primates and physical models Gennarelli and Thibault (1971, 1981, 1982a, 1982b; Thibault & Gennarelli, 1985) reported, angular acceleration as a better predictor for concussive injury, diffuse axonal injury, and subdural hematoma than linear acceleration. Still, manufacturers,

certification standard developers, and policymakers for the most part do not measure head impact severity using rotational acceleration. Assessing how effective linear acceleration is at mirroring deformation to the brain tissue is important.

#### *2.4.3 Brain tissue deformation metrics*

More recent research has suggested that neural injury is more closely tied to the local response of the brain itself and not as much with global input to the head, as measured by kinematic variables. King and colleagues (2003) proposed that the response of brain tissue governs injury, rather than the input acceleration to the head. Accelerations from an impact cause compression, shearing, and other effects on the tissue revealing important information about the resulting injury. This interaction is one of the reasons kinematics-based metrics for brain injury (velocity, linear and rotational acceleration) have been limited in predicting concussive injuries (Goldsmith, 1981). The brain tissue deformation metrics used in the present study were chosen based on research involving cadaveric and animal tissue testing. Axial stretching of neuronal tissues leading to maximum principal strain (MPS) values above 0.14 and von Mises stress values above 8 kPa caused mechanical failure of the tissue (Bain & Meaney, 2000; Anderson et al., 1999). Similarly, research performing reconstructions of injuries identified levels of 0.19 MPS and 7.8 kPa VMS as the threshold for maximum mechanical loading of the tissue before failure in finite element brain models (Kleiven, 2007; Zhang et al., 2004; Willinger & Baumgartner, 2003). MPS and VMS are widely used metrics associated with brain injury. Strain rate has also been used as a biomechanical measure to explain concussion. Strain rate ( $d\epsilon/dt$ ) was calculated by differentiating the MPS vs. time

curves for finite elements within a FE model with the highest strain values (King et al., 2003). Research suggests that strains in excess of 0.10, when applied at greater rates than  $10s^{-1}$ , can cause injury to cells of the brain tissue (Morrison III et al., 2003; Bain & Meaney, 2000; Shreiber et al., 1997). However, Cater et al. (2005) determined from in vivo research that hippocampal cell death was in fact not dependent on strain rate, yet was influenced by the magnitude of strain. This finding suggests that the viscous criterion is not a reliable predictor for injury to brain tissue, at least in the hippocampal region. It should be emphasized that brain tissue deformation variables such as MPS, VMS, and strain rate are modeled variables; they are not synonymous with injury or trauma itself. Although they are highly associated with injury to brain tissue, they have some limitations in terms of the degree that they represent actual tissue damage.

Two-dimensional models were developed by Zhou and colleagues (1994) to simulate the porcine brain, with material properties of the human brain incorporated into it. A rotational impact impulse was applied to the model, resulting in diffuse axonal injury (DAI) in regions where high shear stresses and strains were present for long periods of time. Specifically, strains between 4% and 25%, depending on region of the brain model, resulted in DAI (King et al., 1995).

#### *2.4.4 Thresholds of Injury*

A tolerance level is defined as the magnitude of loading which results in a specific injury at specified injury severity levels (Zhang, 2001). An additional question raised in the research and medical communities is the neural consequences of repetitive trauma such as that

occurring in sports like football. Public concern has begun to surround “sub-concussions”, or repetitive less severe hits that add up over time and potentially contribute to neurodegenerative conditions such as chronic traumatic encephalopathy (Cearnal, 2012). Numerous repeated head impacts may be a reason why linemen in American football may be at increased risk, despite the magnitude of impacts sustained by players in this position being typically lower. Linemen can be exposed to over 1000 impacts per season (Crisco et al., 2010). Research by Schnebel and colleagues (2007) which tracked impacts sustained by high school and college football players while wearing helmets instrumented with the Head Impact Telemetry System showed a clear difference between skilled positions and linemen: skill position players received approximately 25% of all impacts but these were of relatively high magnitude (sustained a  $\geq 98 g$  impact once every 70 impacts), while linemen experienced the greatest number of impacts, most were low magnitude (20-30 *g*) (Schnebel et al., 2007).

Research has been undertaken to define the relationship between biomechanical variables and degree of concussion risk. Zhang, Yang, & King (2004) proposed a method of predicting probability of injury based on shear stress at the brainstem, as shear stress in this region provided the strongest correlation with mTBI. This research also reported thresholds for mTBI based on kinematic variables: translational and rotational acceleration, and the Head Injury Criterion ( $HIC_{15}$ ). Thresholds were proposed for a 25%, 50%, and 80% probability of concussion.

In terms of brain tissue deformation metrics as indicators of mTBI risk, Kleiven (2007) proposed similar distinctions for proportion of injury risk based on MPS. This research suggested a MPS value of 0.26 in the grey matter of the brain and 0.2 in the corpus callosum as

representative of a 50% probability of concussion. Zhang and colleagues (2004) reported a 50% risk of concussion as a MPS of 0.19 in the grey matter. Kleiven also reported this 50% risk level based on a strain rate of  $48.5 \text{ s}^{-1}$ . With respect to the deformation metric of von Mises stress, Kleiven's work reports a 50% probability of concussion as 8.4 kPa, which is comparable to the findings of Zhang et al. 2004 research (7.8 kPa), but lower than what is reported by Willinger and Baumgartner in 2003 (18 kPa). For tissue deformation metrics such as these, thresholds for injury must take into account the region in the brain being considered, as this factor has been shown to account for some variance in injury risk.

*In vivo* tissue models have also been used as a means of determining a strain threshold criterion. Functional injury was delivered by dynamically stretching the optic nerve of a guinea pig to one of seven ocular displacement levels. The authors determined functional impairment to occur when characteristic peaks of visual evoked potentials underwent a latency shift, causing them to occur later than normal. An average Lagrangian strain of  $0.181 (\pm 0.02)$  is reported to be the accepted threshold for electrophysiological, or functional, impairment in a nerve (Bain & Meaney, 2000). In humans, although mechanical injury may not occur at such low strain levels, functional impairment is probable in an *in vivo* context.

#### *2.4.5 Kinematics and brain tissue deformation correlation*

The association of kinematic measures such as peak resultant linear acceleration with brain tissue deformation has been reported in previous research as weak. A discriminant analysis of impacts to a Hybrid III headform showed that peak linear and rotational acceleration did not account for significant variance in maximum principal strain or von Mises

stress. Characteristics of angular acceleration loading curves, however, were shown to more reliably predict deformation in the brain tissue than those of linear acceleration (Post et al., 2012). This is in agreement with the notion that concussion is linked to brain strains, which are correlated with rotational acceleration (Gennarelli, 1971, Forero Rueda et al., 2010; 2011). Ueno and Melvin (1995) showed that linear acceleration of the head had influence over the strain experienced in the brain, and rotational acceleration correlated with shear strains. Contrary to these findings, Forero Rueda and colleagues (2010; 2011) reported low correlation of linear acceleration to brain stress and strain and high correlation of rotational acceleration and these metrics. The precise relationship between tissue response and kinematic variables thus remains ambiguous. However, the interaction between kinematic measures and brain tissue response does appear to be sensitive to tissue type and location. Centric impacts resulted in significantly lower MPS than at non-centric locations. Non-centric impacts are therefore thought to represent a greater risk of injury (Post et al., submitted). Also, centric impacts resulted in a significant correlation between peak linear acceleration and both peak rotational acceleration and MPS (Post et al., 2012).

Location on the head also influences the resulting brain tissue deformation, as different impact sites resulted in different correlations between peak head acceleration and brain deformation metrics. (Post et al., submitted). A hockey helmeted-Hybrid III headform that was impacted according to a centric/non-centric protocol showed a tissue dependent response; the largest magnitudes of stress and strain were found in the grey matter and less in the brainstem and cerebellum (Post et al., 2011).

Peak resultant linear acceleration may not be descriptive enough to predict the magnitude of tissue deformation upon impact. Instead, characteristics of linear and angular acceleration loading curves have been shown to predict brain tissue trauma. One such characteristic which influences the magnitude of brain tissue deformation is the loading curve's time to peak (Post et al., 2012<sup>a</sup>).

## **2.5 Finite Element Modeling**

Finite element analysis (FEA) is a tool that can be used to better understand the mechanisms of head injury. This type of analysis can be used to reveal distribution patterns of stress, strain, or deformation across and within tissues for biomechanical input such as linear and rotational acceleration. Specifically, finite element models of the head were created to represent material properties and complex interactions of neural tissue.

### *2.5.1 University College Dublin Brain Trauma Model*

#### *2.5.1.1 Model development*

The model used in this research was developed in Dublin and is known as the University College Dublin Brain Trauma Model (UCDBTM). The geometric parameters of the model were from a male cadaver and were determined by medical imaging techniques (Horgan and Gilchrist, 2003; Horgan and Gilchrist, 2004; Horgan, 2005). The male head selected was not the size of a 50<sup>th</sup> percentile adult male but was chosen based on the quality of the medical imaging scans. The head and brain finite element model is comprised of ten parts: the scalp, skull (cortical and trabecular bone), pia, falx, tentorium, cerebrospinal fluid

(CSF), grey and white matter, cerebellum and brain stem (Table 1). The scalp was modeled using shell elements, cortical and trabecular bone with brick elements of varying thickness, the dura with membrane elements, CSF with brick elements, pia with membrane elements, falx and tentorium with shell elements and the cerebrum, cerebellum and brain stem with brick elements. The CSF layer was modeled using solid elements with a low shear modulus and a sliding boundary condition between the interfaces of the skull, CSF and brain. The algorithm allowed no spaces between the pia and the CSF layer. For the sliding surfaces a friction coefficient of 0.2 was used (Miller et al., 1998). The fluid present between the falx and the brain and between the tentorium, cerebrum and cerebellum also had the same fluid algorithm. In total, the brain model was comprised of 26,000 elements. The depth of the CSF layer was 1.3 mm to simulate the norm for the average adult male.

#### *2.5.1.2 Material Properties of the Model*

The response of a finite element model is highly dependent on its material properties and characteristics (Bandak and Epperger, 1994). Biological tissues display typically nonlinear behaviours in response to loading. When the material is under compression it generates larger stresses for smaller and smaller strain increments as the body deforms. This behaviour also includes a time dependent effect when applying loading or unloading, which is referred to as viscoelasticity. Linear elastic behaviour occurs when the behaviour in loading and unloading of the material is proportional and the response is instantaneous.

Previous finite element models of the brain have adopted linear elastic material constitutive laws (Shugar and Katona, 1975; Ward and Thompson, 1975). However, the current model uses the parameters used by Mendis et al. (1995) and Kleiven and Von Holst (2002)

which are nonlinear viscoelastic material law under large deformation. A hyperelastic material model was used for the brain in shear in conjunction with the viscoelastic material property.

The hyperelastic law was given by:

$$C_{10}(t) = 0.9C_{01}(t) = 620.5 + 1930e^{-t/0.008} + 1103e^{-t/0.15} \text{ (Pa)} \quad \text{(Equation 1)}$$

where  $C_{10}$  and  $C_{01}$  are the temperature-dependent material parameters, and  $t$  is time in seconds. The compressive behaviour of the brain was considered elastic. The shear characteristics of the viscoelastic behaviour of the brain were expressed by:

$$G(t) = G_{\infty} + (G_0 - G_{\infty})e^{-\beta t} \quad \text{(Equation 2)}$$

where  $G_{\infty}$  is the long term shear modulus,  $G_0$  is the short term shear modulus and  $\beta$  is the decay factor (Horgan and Gilchrist, 2003).

As fluid has a high bulk modulus and zero resistance to shear, the CSF layer was modeled using solid elements with a low shear modulus as was used in other research (Ruan, 1993; Zhou et al., 1995; Kang et al., 1997; Hu et al., 1998; Gilchrist and O'Donoghue, 2000; Gilchrist et al., 2001). This definition creates a near incompressible behaviour for the brain, where small changes in displacement produces large changes in pressure. Although there is a case for some small degree of compressibility of the skull contents, mostly due to CSF shifts into ventricular spaces (Ruan, 1993), the UCDBTM treats brain tissue as incompressible.

The characteristics of brain tissue are those approximated from cadaveric and scaled animal anatomical testing. This is a necessary limitation of models because *in vivo* human brain material parameters do not exist. Cadaver tissue properties are not exactly the same as living tissue, and while *in vivo* testing can be done on animals, the lack of a good scaling law makes

use of this data questionable (Horgan, 2005). Variation can also be created by changes in material properties with age. These limitations to anatomical testing has resulted in there not being a definitive value for the properties of brain tissue, however cadaver tissue represents the closest fit to living human tissue characteristics (Horgan, 2005). From the cadaver testing it has been found that the different parts of brain tissue were heterogeneous as well as having unique geometric arrangement of neural fibers. The material properties for the bone, scalp and intracranial membranes were taken from the literature (Ruan, 1993; Kleiven and von Holst, 2002; Zhou et al., 1996; Willinger et al., 1995) and the values are shown in table 8. The weight of the model was scaled to the dimensions of Nahum et al. (1977) which resulted in a mass of 1.422 kg. Inertial properties are  $I_{yy} = 1795 \text{ kg.mm}^2$ ,  $I_{zz} = 1572 \text{ kg.mm}^2$  and  $I_{xx} = 1315 \text{ kg.mm}^2$ , which are similar to those of Kleiven and von Holst (2002).

**Table 1.** Finite element model material properties

Material	Young's modulus (Mpa)	Poisson's ratio	Density (kg/m <sup>3</sup> )
Scalp	16.7	0.42	1000
Cortical Bone	15000	0.22	2000
Trabecular Bone	1000	0.24	1300
Dura	31.5	0.45	1130
Pia	11.5	0.45	1130
Falx	31.5	0.45	1140
Tentorium	31.5	0.45	1140
CSF	15000	0.5	1000
Grey Matter	Hyperelastic	0.49	1040
White Matter	Hyperelastic	0.49	1040

### *2.5.1.3 Validation of the Model*

Validation of the model was accomplished through comparisons against intracranial pressure data from Nahum et al. (1977) and Trosseille et al. (1992) cadaver impact tests and brain motion against Hardy et al.'s (2001) research. Further validations accomplished comparing real world brain injury events to assess the viability of the model for use for injury assessment (Horgan and Gilchrist, 2003; Horgan and Gilchrist, 2004).

Linear impactor systems consisting of a weighted, pneumatically driven impactor arm; a head- and neckform on a sliding table; and a computerized collection system allow for a greater range of impacting masses and velocities than traditional gravity-driven methods. This, coupled with striker geometry and compliance, affected the amount of energy transferred to the helmet and ultimately the head and brain. The striker used in a centric and non-centric helmet assessment protocol were therefore defined with parameters that mimic realistic impact conditions. Headform impacts were used to assess a variety of striker characteristics in order to establish appropriate apparatus parameters.

An array of impact locations and angles are easily controlled through linear impactors. Small variations in impact angle ( $5^\circ$ ) have been shown to alter the dynamic impact response of a headform across multiple impact locations. By performing a sensitivity analysis of a headform instrumented for three-dimensional impacts and modeling the resulting dynamic impact response using finite element modeling, impact conditions that have brain tissue deformations associated with a high risk of injury could be defined.

#### 2.5.1.4 Research using the University College Dublin Brain Trauma Model

Various research studies have used the UCDBTM to model head injury accidents. Doorly and Gilchrist (2006) reconstructed two cases of injury to the head that occurred as a result of falling. These researchers used multi-body dynamics and the UCD finite element model to accomplish this. The resulting accelerations of the head and brain tissue deformation were in agreement with previously obtained values in the literature. This work demonstrated the usefulness of the UCDBTM for reconstructing real-life injuries. Forero Rueda et al. (2011) also used the UCDBTM to model helmeted rigid headform impacts. These authors found that injury-related loads to brain tissue such as stress or strain were more closely associated with rotational acceleration than with linear acceleration. The limitations of this finite element model were identified, however: it cannot be used to determine a specific injury risk because it needs to be validated against real-world head impacts so injury risk curves can be developed. Still, the UCDBTM can be used to compare between different impacts and to determine the way in which changes in external loads results in changes in neural tissue stress and strain.

## **2.6 Summary**

In this chapter, an overview of the mechanisms of brain injury were described, as well as their predictors and ways in which finite element modeling can further understanding of these injuries by showing the extent and pattern of brain trauma. In football, concussions remain a serious concern. This study aimed to examine the degree to which linear acceleration correlates with brain trauma as measured by brain deformation metrics in football. This

knowledge is useful for designing and certifying football helmets and sensor technology in terms of optimizing preventive efforts to reduce the incidence of head injuries.

## CHAPTER 3

### Methods

#### **3.1 Test Apparatus**

##### *3.1.1 Pneumatic linear impactor*

Helmet-to-helmet injuries with a velocity greater than 5.0 m/s were represented in laboratory testing using the linear impactor. This linear impactor system consisted of a weighted, pneumatically driven impactor arm, a Hybrid III head- and neckform on a sliding table, and a computerized collection system. Similar to a test device created at Wayne State University for the reconstruction of National Football League collision impacts (Pellman et al., 2006), a stationary steel frame secured to a cement floor supported a cylindrical, free-moving impactor arm (length  $1.28 \pm 0.01$  m; mass  $13.1 \pm 0.1$  kg). Consistent system compliance was attained through a hemispherical nylon striker (diameter  $0.132 \pm 0.001$  m; mass  $0.677 \pm 0.001$  kg) containing a vinyl nitrile 602 foam layer (thickness  $0.0357 \pm 0.0001$  m) that caps the impactor arm. The vinyl nitrile cap is designed to reflect the compliance of a helmet to helmet impact.



**Figure 1.** Linear impactor prior to pneumatic release (left); unhelmeted Hybrid III head- and neckform immediately prior to striker contact.

### *3.1.2 Pendulum System*

Elbow or forearm impacts to the head, representing low mass and lower velocity impacts, were simulated using a pendulum system. This pendulum impacting system consisted of a hollow metal frame weighing 3.36 kg (Fig. 2) and is suspended using 3/32" aviation cable (length 9.25 ft.). The impactor was free to swing using four cables attached to ceiling-mounted metal beam directly above the headform. Circular metal plates weighing 1 kg and 2 kg can be fastened into the center of the cylinder to achieve the appropriate mass. When using this system, the Hybrid III head and neck form were attached to a low-friction sliding table. The sliding table ( $12.782 \pm 0.001$  kg) allowed the headform to be adjusted within 6 degrees of freedom, and was mounted on rails to provide a low friction surface. The low friction system allowed the headform to slide upon impact. The pendulum system was positioned so that the impacting end of the metal steel frame was aligned with the impact site on the headform.

Velocity was adjusted by changing the height of the pendulum frame attached by a release magnet. A marker on the pendulum frame acted as a point for digitization of camera footage in order to calculate impact velocity. The marker was tracked 10-15 frames (approximately 7-10 mm) backwards from the point of contact between the VN cap and

helmet. This process provided the displacement of the metal frame of the pendulum prior to impact, which was used to calculate velocity of the impact.

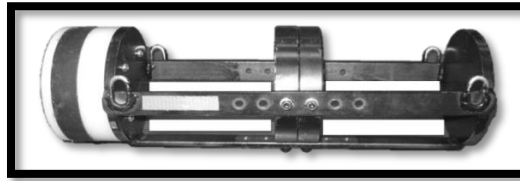


**Figure 2.** Pendulum frame, circular metal weights, and MEP impactor cap

### *3.1.3 Monorail drop system*

To simulate head impacts in football which occurred as a result of falls, a monorail drop rig was used (Figure 3). The head- and neckform attached to the monorail's 4.7 m long rail by means of a special jig. The headform was released by a pneumatic piston, and the pre-established inbound velocity was measured via a photoelectric time gate positioned within 0.02 m of the impact. The anvil at the base of the monorail was modular elastic programmer (MEP) for reconstruction of the falls, as this simulated the ground onto which football players fall.



**Figure 3.** Unhelmeted Hybrid III head and neckform attached to monorail drop rig and impacting a MEP anvil.

### 3.1.4 Hybrid III Head- and Neck Form

For all impacts in this study, a 50<sup>th</sup> percentile adult male Hybrid III head and neckform was used (Figure 4). This headform (mass  $4.54 \pm 0.01$  kg) was instrumented according to Padgaonkar's orthogonal 3-2-2-2 linear accelerometer array protocol (Padgaonkar, 1975). For impacts using the linear impactor and pendulum systems, the complete Hybrid III structure was connected to a sliding table and linear rail system by means of a locking device which is adjustable linearly in all three axes and rotationally in the y- and z-axes. Headform angular acceleration components were calculated based on the first principles of rigid body dynamics and linear accelerations from the orthogonally arranged sensor array:

$$\vec{\alpha}_x = \frac{a_{zS}^{\vec{}} - a_{zC}^{\vec{}}}{2S} - \frac{a_{yT}^{\vec{}} - a_{yC}^{\vec{}}}{2T} \quad (\text{Equation 3})$$

$$\vec{\alpha}_y = \frac{a_{xT}^{\vec{}} - a_{xC}^{\vec{}}}{2T} - \frac{a_{zF}^{\vec{}} - a_{zC}^{\vec{}}}{2F} \quad (\text{Equation 4})$$

$$\vec{\alpha}_z = \frac{a_{yF}^{\vec{}} - a_{yC}^{\vec{}}}{2F} - \frac{a_{xS}^{\vec{}} - a_{xC}^{\vec{}}}{2S} \quad (\text{Equation 5})$$

Where  $\alpha_i$  is the angular acceleration for component  $i$  (x, y, z),  $a_{ij}$  is the linear acceleration for component  $i$  (x, y, z) along orthogonal arm  $j$  (S, T, F) (Padgaonkar, 1975).

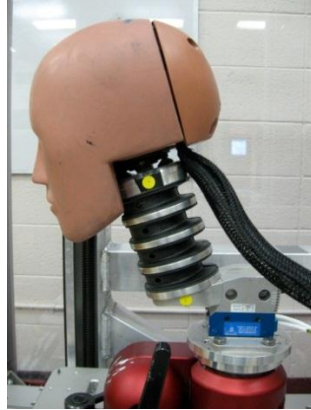


**Figure 4.** Hybrid III head- and neckform mounted on the sliding table.

### *3.1.5 Collection System*

For impacts using the linear impactor system, inbound impactor velocity was measured using an electronic time gate (width  $0.2525 \pm 0.0001$  m) and recorded by computer using National Instruments VI-Logger software. The time gate was validated using a High Speed Imaging PCI-512 Fastcam running at 2 kHz and Photron Motion Tools computer software (Photron, San Diego CA). A variance of three percent from the intended velocity was considered acceptable for the inbound impactor velocity. The nine mounted single-axis Endevco 7264C-2KTZ-2-300 accelerometers (Endevco, San Juan Capistrano CA) were sampled at 20 kHz and filtered using the SAE J211 class 1000 protocol (Society of Automotive Engineers International, 2007). The accelerometer signals were passed through a TDAS Pro Lab system (DTS, Calabasas CA) before being processed by TDAS software. Data collection was triggered when any of the accelerometers reached a 3 g threshold and terminated after 15 ms. This time duration was established using a series of trials with the High Speed Imaging PCI-512 Fastcam synchronized to the TDAS Pro Lab system.

### **3.2 Description of impact conditions**

A summary of the three impact conditions tested is presented in Table 2 below.

#### *3.2.1 Impact velocity*

Representative and realistic inbound impact velocities of each of the three distinct impact mechanisms were obtained from previous research which has reconstructed head impacts from: (i) head to head collisions, (ii) forearm to head strikes, and (iii) falls to the ground. Pellman and colleagues determined that a range of possible head to head impact velocities for football is 3.1 – 11.7 m/s (Pellman et al., 2003). The head to head impact mechanism in the present study was represented by an impact at 11.0 m/s to represent the higher end of these possible impact velocities. Similarly, Withnall and associates measured head kinematics due to upper extremity to head and head to head impacts during football. These researchers reported a range of velocities for head impacts from the hand, wrist, or forearm to be 5.2 to 9.3 m/s (Withnall et al., 2005), so this study performed impacts using the pendulum system at 5.5 m/s to represent arm to head impacts. Research that reconstructed head injuries occurring as a result of falls to the ground described velocities of these impacts to be between 4.0 and 6.2 m/s, for cases that involved the individual falling from a standing height (Post, 2013, submitted). Since football players are typically taller than an average individual, a velocity of 6.0 m/s was used in the present study in order to account for this higher end of the range.

A range of velocities among the three mechanisms was chosen with the intent of maximizing the variance in peak resultant linear head acceleration, thus making the analysis of its correlation with MPS, VMS, and strain rate more robust.

### *3.2.2 Impact Location*

Nine head locations were impacted for each of the three injury mechanisms. These included both centric and non-centric hits, and follow the established University of Ottawa Test Protocol for nine sites (UOTP-9) (Post et al., 2012<sup>b</sup>). This wide variety of locations on the head was impacted to maximize the variation in magnitude of linear acceleration, strengthening the comparison with brain tissue deformation. This protocol also allowed for comparison between centric impacts, which are directed through the head's centre of gravity, and non-centric hits, which occur in a direction other than the head's centre of gravity. In the current study, variations at front, front boss, rear boss, and rear locations of 45° were used as non-centric impact conditions.

### *3.2.3 Impact mechanism*

Head to head impacts were reconstructed using the linear impactor, falls by the monorail drop, and hits to the head by an elbow or forearm by the pendulum. Each of these impact mechanisms also introduced a degree of variation that affect the magnitude of linear acceleration of the head. Specifically, each of these head impact mechanisms typically have different durations; the impact sustained by the head when a player falls to a hard surface is much shorter than a punch to the head, for example.

For the head to head impact mechanism, the following impact parameters were used: a velocity of 11.0 m/s, a mass of 13kg, and compliance represented by vinyl nitrile. For the forearm or elbow to head mechanism, a velocity of 5.5 m/s, a mass of 5.3 kg, and compliance

represented by vinyl nitrile. Lastly, the head to ground mechanism used a 6.0 m/s velocity and the compliance of MEP.

Table 2. Summary of three impact conditions

Head to Head	Head to Ground	Head to forearm/elbow
10.0 m.s	6.0 m/s	5.5 m/s
Linear impactor	Monorail	Pendulum
Vinyl nitrile (VN)	MEP	VN

### 3.3 Procedure

#### 3.3.1 Head Impacts

A total of 81 impacts were performed on a football helmeted, Hybrid III headform. Twenty-seven unique impact conditions were carried out (see section 3.4). A combination of impact mechanisms and corresponding velocity and locations were tested. Each reconstruction was carried out three times to increase the reliability of output data, resulting in the 81 distinct impacts. Each of the three mechanisms by which the struck player was hit incorporated a realistic impacting surface as similar as possible to the helmet, other protective equipment (such as on a forearm or shoulder), or the ground. This impacting surface contacted a regulation American football helmet on the headform in each case, to simulate the struck player.

#### 3.3.2 Finite Element Analysis of Brain Trauma

The resultant dynamic response data (linear and rotational acceleration-time histories) served as input to the finite element model, the UCDBTM. This model was used to

approximate the magnitude and location of MPS, VMS, and strain rate of the brain tissue subjected to each impact .

#### *3.3.2.1 Modification of UCDBTM*

The finite element simulations were run using the University College Dublin Brain Trauma Model (UCDBTM). An element check was done to examine the integrity of the solution based on aspect ratio. The analyses were run to examine the distortion of the elements throughout the simulation time. Elements which showed large deformations (increase in aspect ratio greater than 1.0) in addition to being larger than 3:1 at time zero were identified and excluded from further analyses. Such elements with high aspect ratios were excluded due to resulting in extreme strain results which were deemed to be erroneous. Almost all of the elements which were eliminated were found to be along the tentorium and falx membranes. In total, 217 out of 12,600 elements were excluded.

### **3.4 Research Design**

This research was carried out according to the design outlined in Table 3. The design was a 9 x 3 fully crossed design. For each of the 27 unique impact conditions, peak resultant linear acceleration, MPS, VMS, and strain rate were all measured. This provided an opportunity to look at the degree of correlation among these four variables for each condition. Each of these conditions was tested three times.

**Table 3.** Research Design

	<b>A1</b>	<b>A2</b>	<b>A3</b>
<b>B1</b>	Front PE H-H (11 m/s)	Front PE H-G (6 m/s)	Front PE H-A (5.5 m/s)
<b>B2</b>	Front Boss CG H-H (11 m/s)	Front Boss CG H-G (6 m/s)	Front Boss CG H-A (5.5 m/s)
<b>B3</b>	Front Boss PA H-H (11 m/s)	Front Boss PA H-G (6 m/s)	Front Boss PA H-A (5.5 m/s)
<b>B4</b>	Side CG H-H (11 m/s)	Side CG H-G (6 m/s)	Side CG H-A (5.5 m/s)
<b>B5</b>	Rear Boss NA H-H (11 m/s)	Rear Boss NA H-G (6 m/s)	Rear Boss NA H-A (5.5 m/s)
<b>B6</b>	Rear Boss CG H-H (11 m/s)	Rear Boss CG H-G (6 m/s)	Rear Boss CG H-A (5.5 m/s)
<b>B7</b>	Rear NA H-H (11 m/s)	Rear NA H-G (6 m/s)	Rear NA H-A (5.5 m/s)
<b>B8</b>	Rear CG H-H (11 m/s)	Rear CG H-G (6 m/s)	Rear CG H-A (5.5 m/s)
<b>B9</b>	Front FG H-H (11 m/s)	Front FG H-G (6 m/s)	Front FG H-A (5.5 m/s)

Where A and B = independent variables:

A = Mechanism of impact

A1 = Head to head (**H-H**); at 11.0 m/s

A2 = Head to ground (**H-G**); at 6.0 m/s

A3 = Forearm to head (**H-A**); at 5.5 m/s.

B = Impact location

B1 = Front Positive Elevation 15°

B2 = Front Boss Centre of Gravity

B3 = Front Boss Positive Azimuth

B4 = Side Centre of Gravity

B5 = Rear Boss Negative Azimuth

B6 = Rear Boss Centre of Gravity

B7 = Rear Negative Azimuth

B8 = Rear Centre of Gravity

B9 = Front Faceguard

Independent variables:

(i) Impact mechanism (3 levels: head to head, forearm to head, head to ground)

(ii) Impact condition (9 levels: UOTP<sup>9</sup> protocol)

Dependent variables:

*Finite element-modeled brain tissue deformation:*

(i) Peak resultant linear acceleration ( $g$ );

(ii) Maximum principal strain;

(iii) von Mises stress (Pa);

(iv) Strain rate ( $s^{-1}$ ).

### **3.6 Statistical Analysis**

To determine the degree of association between peak resultant linear acceleration and MPS, VMS, and strain rate, Pearson product-moment correlation coefficients ( $r$ ) were calculated. Assumptions that were made in order to use this statistic are as follows: that all variables are continuous variables measured on interval or ratio scales; that the linear (not

curvilinear) relationship was measured; and that the variables are normally distributed. When  $r$  was calculated using the statistical software, the  $p$  value of significance was determined for each correlation. In this study, alpha was set at  $p < 0.05$ . In the present study, Pearson correlation coefficients ( $r$ ) was determined for each mechanism of injury and impact location, as well as for all mechanisms together.

## CHAPTER 4

### Results

The objective of this study was to investigate the degree to which peak resultant linear acceleration of the head is associated with the injury-related parameters of MPS, VMS, and strain rate. This relationship was examined under twenty-seven distinct impact conditions. Impacts to the head characteristic of those occurring in the sport of American football were performed according to three mechanisms of impact and nine locations on the head. Impacts were repeated three times for each condition for a total of 81 impacts. A range of linear acceleration was established by the varying velocity, mass, head location, and compliance of each of the impact conditions in order to investigate whether the correlation with each of the tissue deformation metrics remained consistent or whether it was dependent on any of these parameters.

Results for each of the four dependent variables, peak resultant linear acceleration, maximum principal strain, von Mises stress, and strain rate, are presented in tables 3-6 below. Averaged results across the three trials for each unique condition (location on the head and mechanism of impact) are presented.

**Table 4.** Peak resultant linear acceleration results in *g*; (average of three trials of each condition; standard deviation indicated in parentheses)

	<b>Head-Head</b>	<b>Arm-Head</b>	<b>Falls</b>
<b>Front Boss CG</b>	119.13 (0.26)	57.30 (5.11)	111.73 (7.26)
<b>Front Boss Positive Azimuth</b>	142.83 (11.97)	39.30 (1.02)	137.53 (8.21)
<b>Front Faceguard</b>	90.10 (6.64)	39.60 (0.41)	73.60 (7.81)
<b>Front Positive Elevation 15°</b>	105.70 (4.27)	50.07 (1.54)	133.97 (7.72)
<b>Side CG</b>	138.13 (12.5)	35.63 (2.29)	120.93 (4.49)
<b>Rear Boss CG</b>	144.8 (1.3)	32.33 (0.41)	118.43 (1.86)
<b>Rear Boss Negative Azimuth</b>	146 (7.15)	32.5 (0)	122.33 (9.39)
<b>Rear CG</b>	158.83 (6.73)	35.33 (0.31)	181.2 (26.66)
<b>Rear Negative Azimuth</b>	148.03 (1.79)	31.87 (1.37)	134.5 (22.53)
<b>Average for all locations</b>	<b>132.62</b>	<b>34.93</b>	<b>126.02</b>

**Table 5.** Maximum principal strain results (average of three trials of each condition; standard deviation indicated in parentheses)

	<b>Head-Head</b>	<b>Arm-Head</b>	<b>Falls</b>
<b>Front Boss CG</b>	0.550 (0.009)	0.273 (0.019)	0.609 (0.021)
<b>Front Boss Positive Azimuth</b>	0.588 (0.044)	0.13 (0.099)	0.305 (0.223)
<b>Front Faceguard</b>	0.452 (0.041)	0.204 (0.004)	0.360 (0.035)
<b>Front Positive Elevation 15°</b>	0.459 (0.007)	0.172 (0.017)	0.468 (0.012)
<b>Side CG</b>	0.631 (0.048)	0.239 (0.008)	0.537 (0.015)
<b>Rear Boss CG</b>	0.719 (0.017)	0.183 (0.008)	0.481 (0.017)
<b>Rear Boss Negative Azimuth</b>	0.791 (0.009)	0.228 (0.000)	0.451 (0.024)
<b>Rear CG</b>	0.532 (0.301)	0.142 (0.003)	0.539 (0.09)
<b>Rear Negative Azimuth</b>	0.644 (0.036)	0.154 (0.005)	0.476 (0.135)
<b>Average for all locations</b>	<b>0.596</b>	<b>0.192</b>	<b>0.4696</b>

**Table 6.** Von Mises stress results in Pa (average of three trials of each condition; standard deviation indicated in parentheses)

	<b>Head-Head</b>	<b>Arm-Head</b>	<b>Falls</b>
<b>Front Boss CG</b>	17285.4 (879.4)	8122.83 (467.6)	18449.37 (752.6)
<b>Front Boss Positive Azimuth</b>	19435.83 (1641.8)	5044.9 (379.2)	9165.86 (7089.6)
<b>Front Faceguard</b>	11401.43 (1279.0)	4814.25 (307.0)	9981.79 (760.2)
<b>Front Positive Elevation 15°</b>	12217 (411.8)	4697.61 (536.6)	12835.53 (115.1)
<b>Side CG</b>	19927.73 (936.7)	8118.25 (182.2)	16434.47 (543.0)
<b>Rear Boss CG</b>	23929.3 (889.6)	6221.79 (484.7)	16533.8 (1187.7)
<b>Rear Boss Negative Azimuth</b>	26475.43 (3017.6)	6234.58 (32.0)	13703.2 (939.2)
<b>Rear CG</b>	23066.53 (1562.9)	4056.97 (215.7)	17571.87 (3759.5)
<b>Rear Negative Azimuth</b>	25063.2 (1607.7)	4942.77 (226.7)	15602.8 (2692.4)
<b>Average for all locations</b>	<b>19866.87</b>	<b>5805.99</b>	<b>14475.41</b>

**Table 7.** Strain rate results in  $s^{-1}$  (average of three trials of each condition; standard deviation indicated in parentheses)

	<b>Head-Head</b>	<b>Arm-Head</b>	<b>Falls</b>
<b>Front Boss CG</b>	151.86 (0.27)	72.41 (3.95)	169.02 (6.43)
<b>Front Boss Positive Azimuth</b>	168.79 (22.67)	58.15 (24.85)	102.25 (35.0)
<b>Front Faceguard</b>	146.818 (60.16)	208.98 (71.66)	118.06 (7.9)
<b>Front Positive Elevation 15°</b>	164.54 (23.79)	150.55 (105.37)	214.19 (56.82)
<b>Side CG</b>	206.31 (40.40)	65.31 (3.94)	149.46 (6.3)
<b>Rear Boss CG</b>	199.6 (13.48)	40.02 (2.31)	80.07 (69.34)
<b>Rear Boss Negative Azimuth</b>	246.11 (33.87)	127.23 (86.23)	121.74 (21.98)
<b>Rear CG</b>	175.3 (101.66)	81.10 (9.86)	222.40 (53.4)
<b>Rear Negative Azimuth</b>	308.369 (3.87)	57.21 (18.0)	129.39 (57.53)
<b>Average for all locations</b>	<b>196.411</b>	<b>95.662</b>	<b>145.176</b>

#### 4.1 Correlation with maximum principal strain

A range of linear acceleration values was established by performing impacts representative of various mechanisms and locations on the head commonly occurring in

American football. Within this range, the correlation between peak resultant linear acceleration and peak maximum principal strain (MPS) in the cerebrum was determined. Table 4 presents the average MPS for each impact mechanism overall. Table 7 shows the results of the statistical analysis of this correlation across each impact mechanism as well as all mechanisms combined. A statistically significant Pearson product-moment correlation coefficient of  $r = 0.824$  was calculated for the overall correlation between linear acceleration and MPS for all mechanisms ( $p = 6.73 \times 10^{-21}$ ). Similarly,  $r = 0.477$ ,  $0.394$ ,  $0.360$  represent the strength of this correlation for head to head, arm or elbow to head, and falling impacts respectively. However, only the correlation coefficient for head to head impacts was significant ( $p = 0.012$ ).

The correlations of peak resultant linear acceleration with MPS for each of the nine tested locations on the head, with all impact mechanisms combined, are shown in Table 8. The Pearson product-moment correlation coefficients for the centric impact locations were  $r = 0.936$ ,  $0.951$ ,  $0.996$ ,  $0.969$ ,  $0.759$ ,  $0.985$  for front positive elevation  $15^\circ$ , front boss centre gravity, side centre gravity, rear boss centre gravity, rear centre gravity, and front faceguard respectively. The average correlation coefficient was  $r = 0.933$  for these centric locations. The strength of the correlation between linear acceleration and MPS for non-centric impact locations was shown by  $r = 0.738$ ,  $0.866$ ,  $0.967$  for front boss positive azimuth, rear boss negative azimuth, and rear negative azimuth respectively. The average strength of the correlation for non-centric impact locations was  $r = 0.857$ . Thus, the hypothesis that linear acceleration and MPS would be minimally correlated with one another across all impact locations and mechanisms ( $r < 0.5$ ) was rejected.

**Table 8.** Pearson correlations between linear acceleration and MPS by impact mechanism

			<b>Peak MPS</b>
Head to head impacts	<b>Linear Acceleration</b>	Pearson correlation coefficient	<b>0.477*</b>
		Sig. (2-tailed)	0.012
Forearm / elbow to head impacts	<b>Linear Acceleration</b>	Pearson correlation coefficient	<b>0.394</b>
		Sig. (2-tailed)	0.052
Falls to ground	<b>Linear Acceleration</b>	Pearson correlation coefficient	<b>0.360</b>
		Sig. (2-tailed)	0.065
All mechanisms	<b>Linear Acceleration</b>	Pearson correlation coefficient	<b>0.824*</b>
		Sig. (2-tailed)	< 0.005

**Table 9.** Pearson correlations between linear acceleration and MPS by impact location

FPE15	<b>Linear Acceleration</b>	Pearson correlation coefficient Sig. (2-tailed)	<b>Peak MPS</b> 0.936** < 0.005
FBCG	<b>Linear Acceleration</b>	Pearson correlation coefficient Sig. (2-tailed)	<b>Peak MPS</b> 0.951** < 0.005
FBPA	<b>Linear Acceleration</b>	Pearson correlation coefficient Sig. (2-tailed)	<b>Peak MPS</b> 0.738* 0.023
SCG	<b>Linear Acceleration</b>	Pearson correlation coefficient Sig. (2-tailed)	<b>Peak MPS</b> 0.996** < 0.005
RBCG	<b>Linear Acceleration</b>	Pearson correlation coefficient Sig. (2-tailed)	<b>Peak MPS</b> 0.969** < 0.005
RBNA	<b>Linear Acceleration</b>	Pearson correlation coefficient Sig. (2-tailed)	<b>Peak MPS</b> 0.866** 0.005
RCG	<b>Linear Acceleration</b>	Pearson correlation coefficient Sig. (2-tailed)	<b>Peak MPS</b> 0.759* 0.018
RNA	<b>Linear Acceleration</b>	Pearson correlation coefficient Sig. (2-tailed)	<b>Peak MPS</b> 0.967** < 0.005
FFG	<b>Linear Acceleration</b>	Pearson correlation coefficient Sig. (2-tailed)	<b>Peak MPS</b> 0.985** < 0.005

Scatterplots of the relationship between linear acceleration and MPS for each mechanism of injury individually are presented in Figures 5-7. Figure 8 shows a scatterplot of

the relationship for all mechanisms combined. As the three impact mechanisms are designated by the different colours, the relationship between linear acceleration and MPS in the cerebrum stays relatively consistent across the head impact mechanisms, apart from a few outlier data points. For example, as MPS increases, so does linear acceleration. Due to different energy levels of the impacts of each mechanism however, three clusters of data emerged. Arm or elbow strikes to the head resulted in the lowest linear acceleration of the head and MPS in the cerebrum. There was some overlap for the magnitudes of linear acceleration and MPS between the impacts representing falls and head to head collisions. The results for falls were more variable than for the other two mechanisms, particularly in the way that these impacts resulted in a wider range of linear acceleration. As a whole however, falls resulted in slightly lower values than the head to head impacts carried out in this study.

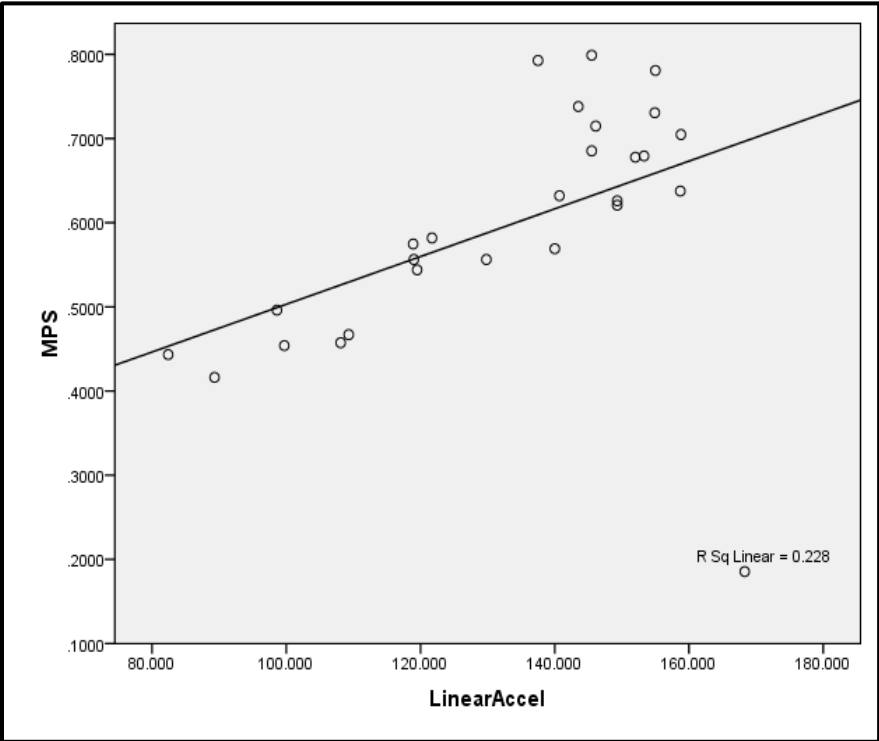


**Figure 5.** Scatterplot of peak linear acceleration versus maximum principal strain for head to head impact mechanism

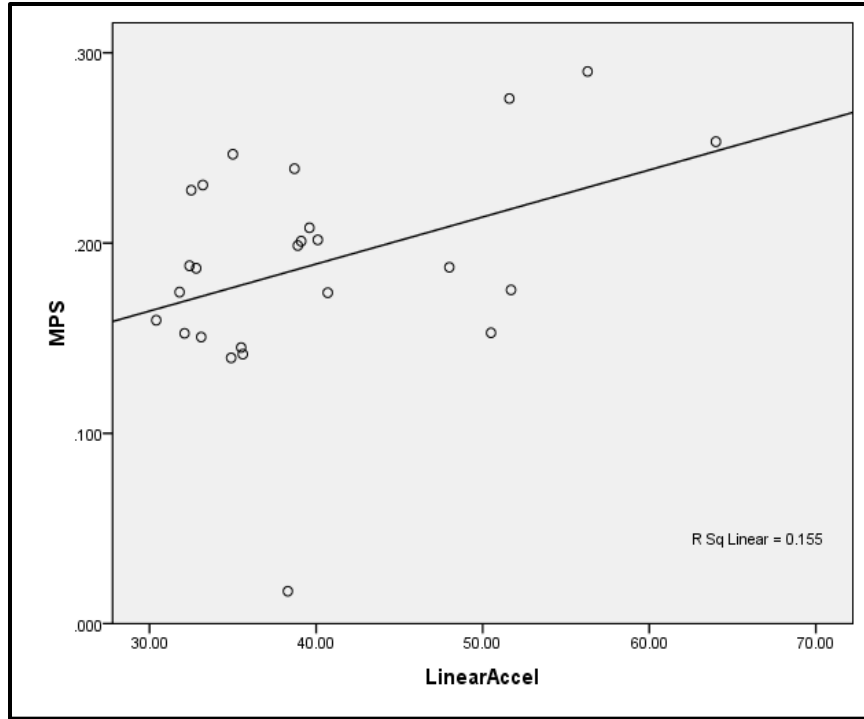


**Figure 6.** Scatterplot of peak linear acceleration versus maximum principal strain for arm to head impact mechanism

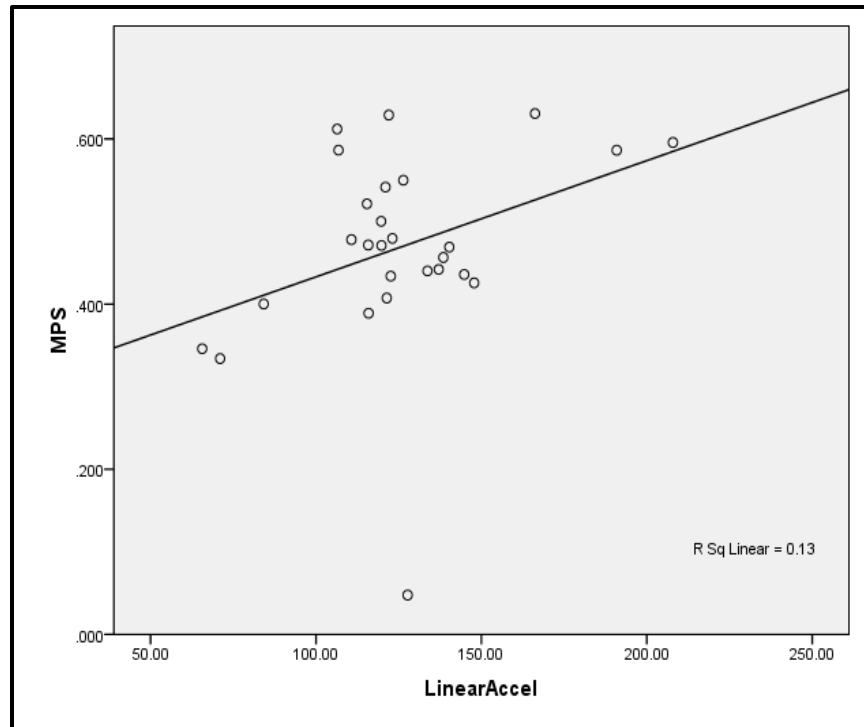


**Figure 7.** Scatterplot of peak linear acceleration versus maximum principal strain for fall impact mechanism

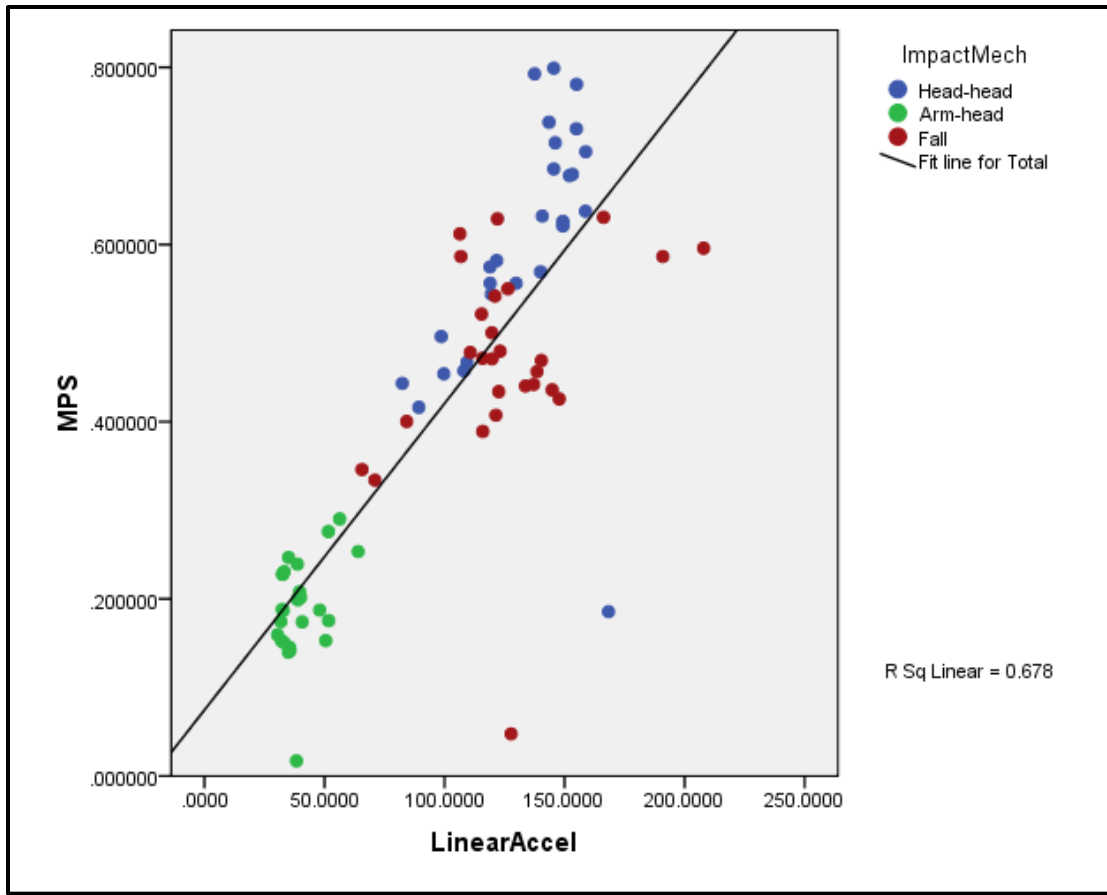


**Figure 8.** Scatterplot of peak linear acceleration versus maximum principal strain for all impact mechanisms

#### 4.2 Correlation with von Mises stress

The correlation between linear acceleration and peak VMS in the cerebral tissue, as measured by finite element modeling, followed a similar but not identical trend to the correlation of linear acceleration with MPS. Table 9 shows the results of the correlation between these two variables for each of the impact mechanisms individually as well as for all three mechanisms combined. A significant Pearson product-moment correlation coefficient of 0.858 described the correlation between linear acceleration and VMS for head to head impacts

( $p = 1.03 \times 10^{-8}$ ). The correlation for impacts representative of falling to the ground was also statistically significant at  $r = 0.42$  ( $p = 0.029$ ). The correlation coefficient indicating the magnitude of this association for forearm or elbow to head impacts was lower,  $r = 0.272$ , and was not significant ( $p = 0.189$ ). For all three mechanisms of head impacts combined, the strength of the correlation between linear acceleration and VMS was  $r = 0.852$  ( $p < 0.005$ ).

The correlations of peak resultant linear acceleration with VMS for each of the nine tested locations on the head, with all impact mechanisms combined, are shown in Table 10. The Pearson product-moment correlation coefficients for the centric impact locations were  $r = 0.950, 0.962, 0.987, 0.419, 0.905, 0.969$  for front positive elevation  $15^\circ$ , front boss centre gravity, side centre gravity, rear boss centre gravity, rear centre gravity, and front faceguard respectively. The average correlation coefficient was  $r = 0.865$  for centric locations. The strength of the correlation between linear acceleration and VMS for non-centric impact locations was shown by  $r = 0.699, 0.832, 0.921$  for front boss positive azimuth, rear boss negative azimuth, and rear negative azimuth respectively. The average strength of the correlation for non-centric impact locations was  $r = 0.817$ . Therefore, the hypothesis that linear acceleration and VMS would have a low positive correlation ( $r < 0.5$ ) for all mechanisms and locations was rejected.

**Table 10.** Pearson correlations between linear acceleration and VMS by impact mechanism

			<b>Peak VMS</b>
Head to head impacts	<b>Linear Acceleration</b>	Pearson correlation coefficient Sig. (2-tailed)	<b>0.858*</b> < 0.005
Forearm / elbow to head impacts	<b>Linear Acceleration</b>	Pearson correlation coefficient Sig. (2-tailed)	<b>0.272</b> 0.189
Falls to ground	<b>Linear Acceleration</b>	Pearson correlation coefficient Sig. (2-tailed)	<b>0.420*</b> 0.029
All mechanisms	<b>Linear Acceleration</b>	Pearson correlation coefficient Sig. (2-tailed)	<b>0.852*</b> < 0.005

**Table 11.** Pearson correlations between linear acceleration and VMS by impact location

FPE15	<b>Linear Acceleration</b>	Pearson correlation coefficient Sig. (2-tailed)	<b>Peak MPS</b> 0.950** < 0.005
FBCG	<b>Linear Acceleration</b>	Pearson correlation coefficient Sig. (2-tailed)	<b>Peak MPS</b> 0.962** < 0.005
FBPA	<b>Linear Acceleration</b>	Pearson correlation coefficient Sig. (2-tailed)	<b>Peak MPS</b> 0.699* 0.036
SCG	<b>Linear Acceleration</b>	Pearson correlation coefficient Sig. (2-tailed)	<b>Peak MPS</b> 0.987** < 0.005
RBCG	<b>Linear Acceleration</b>	Pearson correlation coefficient Sig. (2-tailed)	<b>Peak MPS</b> 0.419 0.301
RBNA	<b>Linear Acceleration</b>	Pearson correlation coefficient Sig. (2-tailed)	<b>Peak MPS</b> 0.832* 0.01
RCG	<b>Linear Acceleration</b>	Pearson correlation coefficient Sig. (2-tailed)	<b>Peak MPS</b> 0.905** 0.001
RNA	<b>Linear Acceleration</b>	Pearson correlation coefficient Sig. (2-tailed)	<b>Peak MPS</b> 0.921** < 0.005
FFG	<b>Linear Acceleration</b>	Pearson correlation coefficient Sig. (2-tailed)	<b>Peak MPS</b> 0.969** < 0.005

The relationship between linear acceleration and VMS across all three mechanisms of impact is summarized in the scatterplot shown in Figure 12 and presented for each mechanism

individually in figures 9-11. Similar to the relationship between linear acceleration and MPS, the correlation with VMS remained relatively similar across the three head impact mechanisms. Also like the correlation of linear acceleration with MPS, clustering of the data according to the inbound energy of the impacts was noted, with head to head impacts having the highest linear acceleration and VMS, and forearm to head impacts having the lowest measures of both variables, with the results for falls to the ground lying between the two. However, separation of the results for each impact mechanism from one another occurred to a greater degree for VMS than the results for MPS. Overall, there was a strong, positive correlation between VMS in the cerebrum and peak resultant linear acceleration, but only for head to head collisions. For falls and forearm to head impacts, the variables showed low to moderate positive correlations.

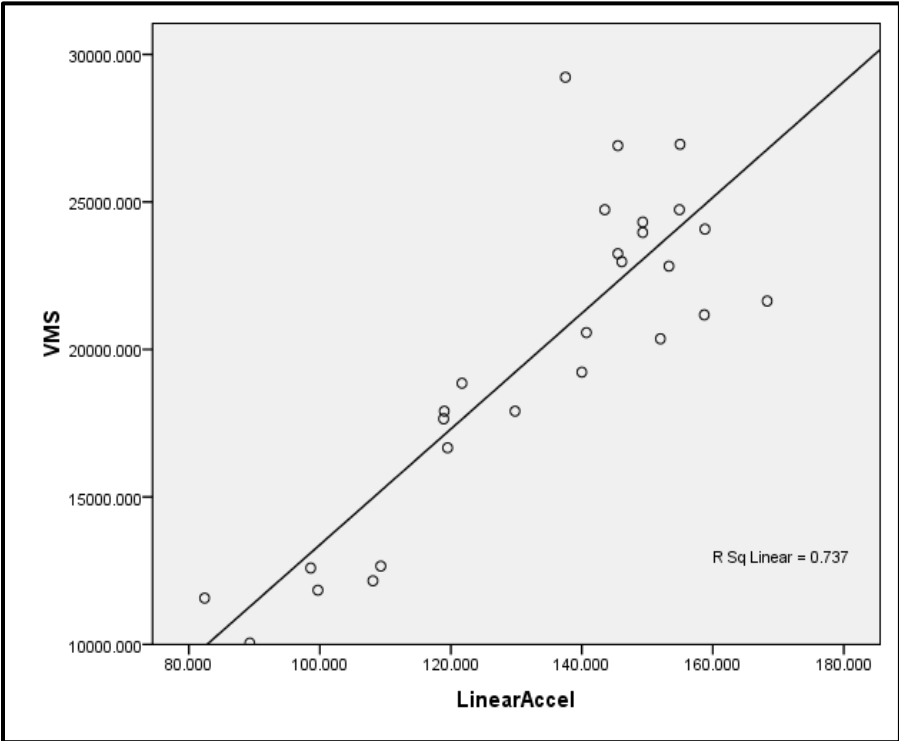


**Figure 9.** Scatterplot of peak linear acceleration versus von Mises stress for head to head impact mechanism

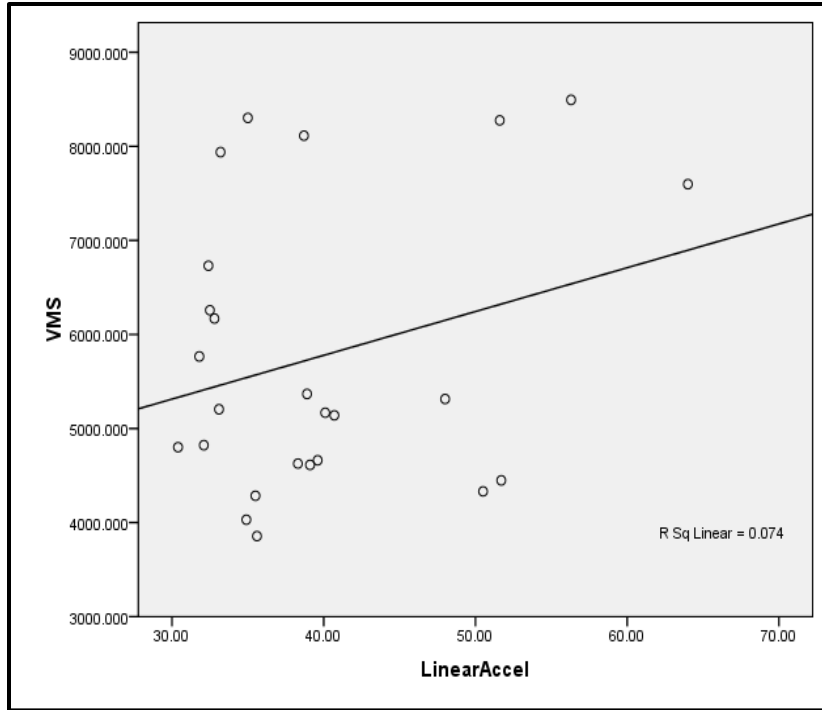


**Figure 10.** Scatterplot of peak linear acceleration versus von Mises stress for arm to head impact mechanism

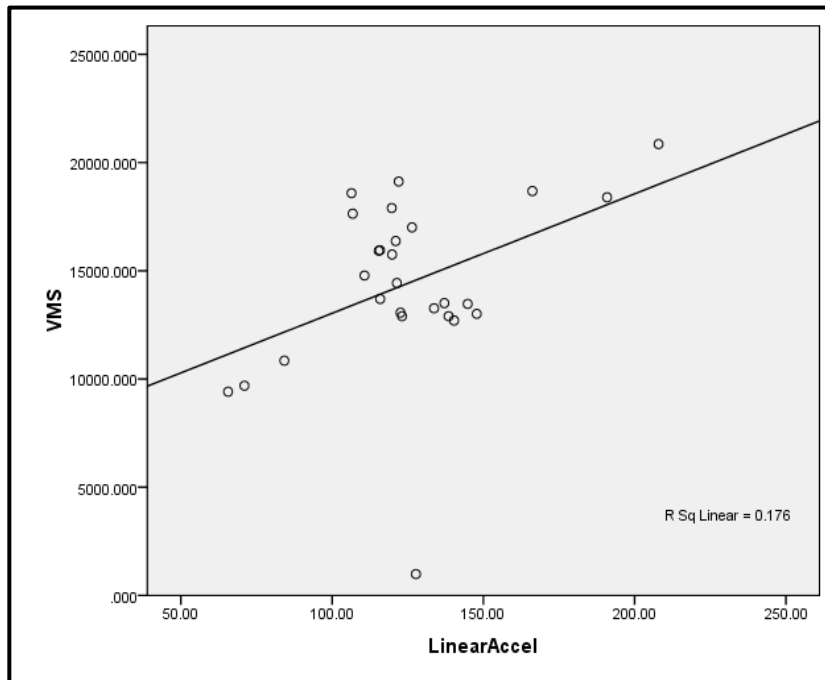


**Figure 11.** Scatterplot of peak linear acceleration versus von Mises stress for fall impact mechanism

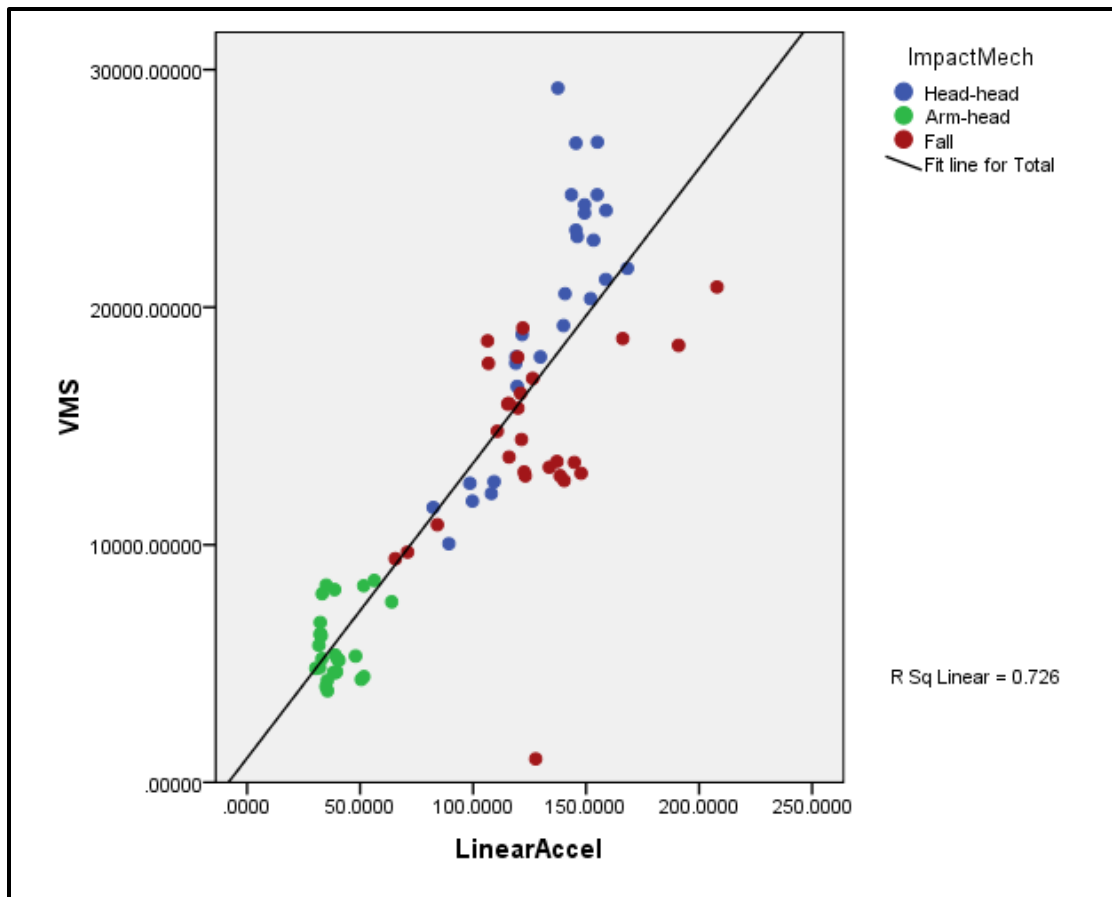


**Figure 12.** Scatterplot of peak linear acceleration versus von Mises stress for all impact mechanisms

#### 4.3 Correlation with strain rate

The correlation of linear acceleration with strain rate is summarized in Table 11, with the results separated by impact mechanism in addition to the relationship for all mechanisms combined. The association between peak linear acceleration and this metric for brain tissue deformation was quantified by a statistically significant Pearson product-moment correlation of  $r = 0.424$  for head to head collisions specifically ( $p = 0.027$ ). The correlation for impacts representative of falling to the ground was also statistically significant at  $r = 0.42$  ( $p = 0.029$ ). The correlation coefficient indicating the magnitude of this association for forearm or elbow to

head impacts was lower,  $r = 0.272$ , and was not significant ( $p = 0.189$ ). For all three mechanisms of head impacts combined, the strength of the correlation between linear acceleration and strain rate was  $r = 0.585$  ( $p < 0.005$ ).

The correlations of peak resultant linear acceleration with strain rate for each of the nine tested locations on the head, with all impact mechanisms combined, are shown in Table 12. The Pearson product-moment correlation coefficients for the centric impact locations were  $r = 0.321, 0.950, 0.955, 0.708, 0.801, -0.469$  for front positive elevation  $15^\circ$ , front boss centre gravity, side centre gravity, rear boss centre gravity, rear centre gravity, and front faceguard respectively. The average correlation coefficient was  $r = 0.701$  for these centric locations. The strength of the correlation between linear acceleration and MPS for non-centric impact locations was shown by  $r = 0.776, 0.518, 0.801$ , for front boss positive azimuth, rear boss negative azimuth, and rear negative azimuth respectively. The average strength of the correlation for non-centric impact locations was  $r = 0.698$ . Therefore, the hypothesis that linear acceleration and strain rate would have a low positive correlation ( $r < 0.5$ ) for all mechanisms and locations was rejected.

**Table 12.** Pearson correlations between linear acceleration and strain rate by impact mechanism

			<b>Peak Strain Rate</b>
Head to head impacts	<b>Linear Acceleration</b>	Pearson correlation coefficient	<b>0.424*</b>
			0.027
		Sig. (2-tailed)	
Forearm / elbow to head impacts	<b>Linear Acceleration</b>	Pearson correlation coefficient	<b>0.165</b>
			0.431
		Sig. (2-tailed)	
Falls to ground	<b>Linear Acceleration</b>	Pearson correlation coefficient	<b>0.495*</b>
			0.009
		Sig. (2-tailed)	
All mechanisms	<b>Linear Acceleration</b>	Pearson correlation coefficient	<b>0.585*</b>
			< 0.005
		Sig. (2-tailed)	

**Table 13.** Pearson correlations between linear acceleration and strain rate by impact location

FPE15	<b>Linear Acceleration</b>	Pearson correlation coefficient Sig. (2-tailed)	<b>Peak MPS</b> 0.321 0.4
FBCG	<b>Linear Acceleration</b>	Pearson correlation coefficient Sig. (2-tailed)	<b>Peak MPS</b> 0.950** < 0.005
FBPA	<b>Linear Acceleration</b>	Pearson correlation coefficient Sig. (2-tailed)	<b>Peak MPS</b> 0.776* 0.014
SCG	<b>Linear Acceleration</b>	Pearson correlation coefficient Sig. (2-tailed)	<b>Peak MPS</b> 0.955 < 0.005
RBCG	<b>Linear Acceleration</b>	Pearson correlation coefficient Sig. (2-tailed)	<b>Peak MPS</b> 0.708* 0.049
RBNA	<b>Linear Acceleration</b>	Pearson correlation coefficient Sig. (2-tailed)	<b>Peak MPS</b> 0.518 0.188
RCG	<b>Linear Acceleration</b>	Pearson correlation coefficient Sig. (2-tailed)	<b>Peak MPS</b> 0.732* 0.025
RNA	<b>Linear Acceleration</b>	Pearson correlation coefficient Sig. (2-tailed)	<b>Peak MPS</b> 0.801** 0.01
FFG	<b>Linear Acceleration</b>	Pearson correlation coefficient Sig. (2-tailed)	<b>Peak MPS</b> -0.469 0.203

The association of linear acceleration with strain rate for all mechanisms combined is summarized in Figure 16 and shown for each mechanism individually in figures 13-15. Unlike

the correlation of this kinematic variable with MPS and VMS, increases in linear acceleration do not result in increases in strain rate to the same extent. This observation holds true across all three impact mechanisms. Related to this, much less separation of the data of each impact mechanism into discrete clusters was observed for the relationship between these two variables. Unlike what is seen in the scatterplots of the relationships of linear acceleration with MPS and VMS, overlap occurred among all of the impact mechanisms. Overall, a low, positive correlation existed between strain rate and peak resultant linear acceleration for all of the impact mechanisms individually. However, when all three mechanisms were analyzed as a whole, there was a moderate positive correlation of strain rate with linear acceleration.

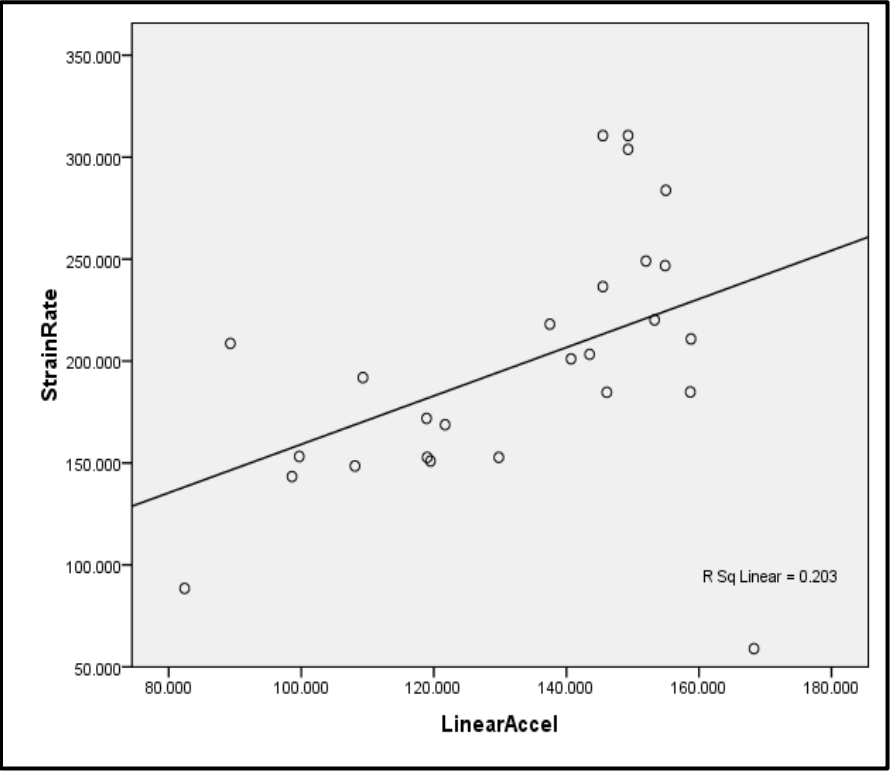


**Figure 13.** Scatterplot of peak linear acceleration versus strain rate for head to head impact mechanism

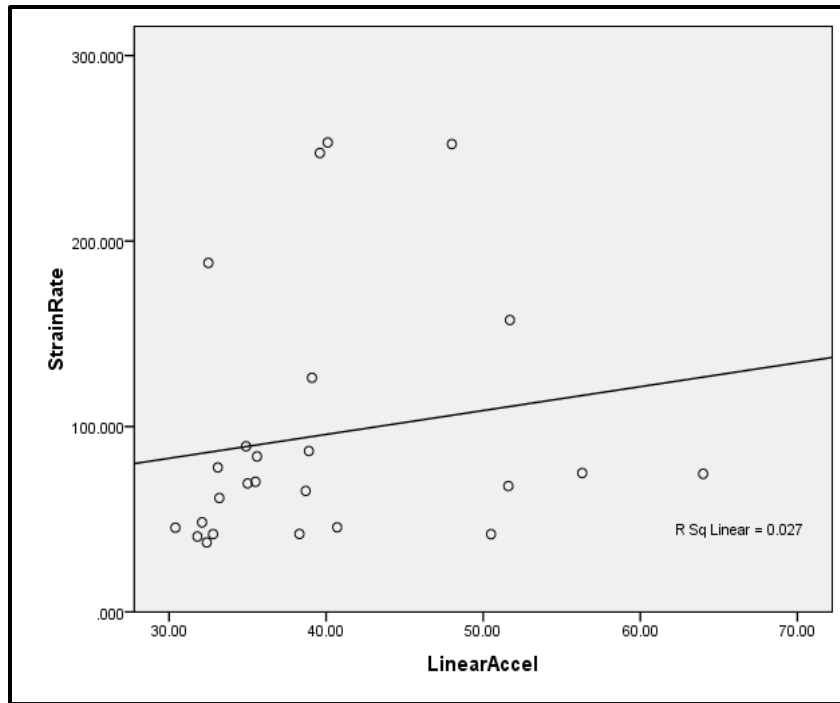


**Figure 14.** Scatterplot of peak linear acceleration versus strain rate for arm to head impact mechanism

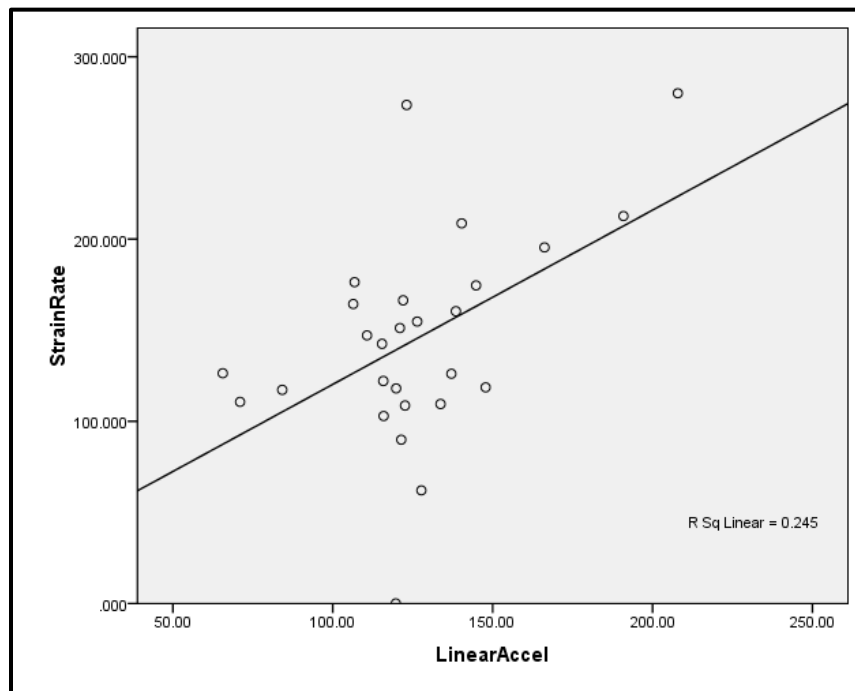


**Figure 15.** Scatterplot of peak linear acceleration versus strain rate for fall impact mechanism

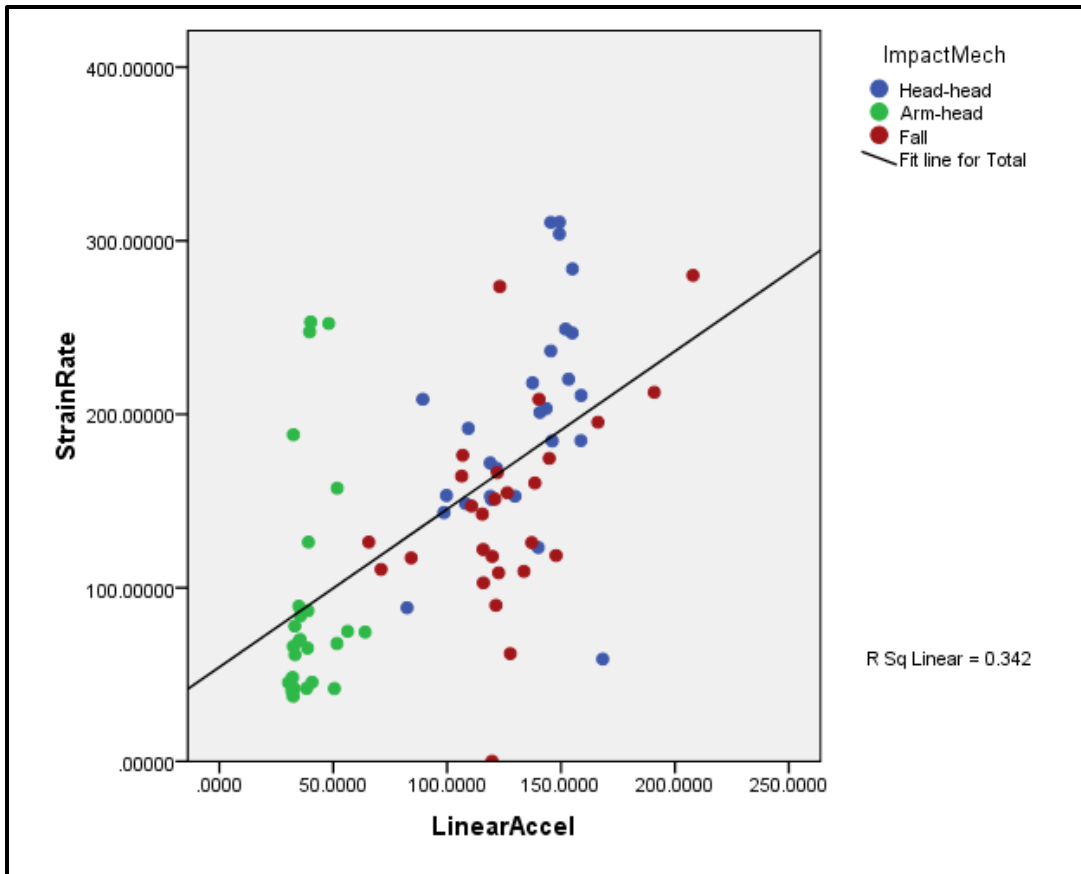


**Figure 16.** Scatterplot of peak linear acceleration versus strain rate for all impact mechanisms

## CHAPTER 5

### Discussion

Understanding the relationship between peak resultant linear acceleration and stress- and strain-based metrics of injury has important implications for developing head protection in sport. Strong and reliable correlations between peak resultant linear acceleration and the deformation response of brain tissue would allow accelerometer-instrumented headforms to approximate the response of brain tissue trauma to an impact. However, the lack of consistent associations between these parameters would indicate a limitation in the ability of linear acceleration, to represent brain tissue loading.

#### **5.1 Correlation of linear acceleration with brain tissue deformation metrics**

The extent to which linear acceleration is associated with brain tissue deformation-related measures of trauma was investigated for three metrics that have been shown to be linked to injury: MPS, VMS, and strain rate (Forero Rueda, Cui, & Gilchrist, 2011). In terms of the relationship between peak resultant linear acceleration of the head and peak MPS in the cerebrum, a significant correlation between the two variables was found for the head to head impact. This relationship was of moderate strength ( $r = 0.477$ ); however, when all three mechanisms of impact were considered together, there was a significant strong, positive correlation ( $r = 0.824$ ). No significant association of linear acceleration was found with MPS for forearm or elbow to head impacts or head impacts occurring due to falls.

Due to high velocity and higher mass, head to head impacts had the highest inbound energy compared to impacts representing the other two mechanisms. One explanation for linear acceleration and MPS correlated only for head to head collisions is that high magnitudes of inbound energy may result in linear acceleration being moderately effective at representing strain in the brain tissue. Lower impact energies, such as impacts from falls and the forearm or elbow to head impacts, allow for the difference between linear acceleration and MPS to become evident. In particular, the impacts to representing head to head collisions had a velocity at the high end of the range at which impacts of this type occur in real-life football. It has been reported that 67% of head impacts in American football occur as a result of two players hitting their heads together (Pellman et al., 2004). However, the majority of all head to head impacts in football, when considering the average age and abilities of all football players, likely do not occur with as high an energy level as used in this study.

The strength of the correlation between linear acceleration and MPS determined in this study differed from previous research investigating the relationship between these two variables. Forero Rueda et al. (2011) report the correlation coefficient for the relationship between linear acceleration and MPS to be 0.2 for simulated helmeted rigid headform impacts. However, they note a high correlation of rotational acceleration with stress and strain in the brain tissue (0.72). Post et al. (2011) impacted a helmeted Hybrid III headform and obtained values of MPS and VMS via finite element modeling. They report a low negative correlation of peak resultant linear acceleration and MPS (-0.239) for the brain tissue global response. Thus, the current study's results of the correlation between linear acceleration and MPS was notably higher than Post et al.; this could be due to differences in the impact

protocol to the Hybrid III headform. These authors impacted only five sites on the headform, and performed the impacts with the linear impactor only, instead of using multiple types of equipment to replicate multiple mechanisms of impact. Additionally, Post and colleagues performed the impacts to the headform outfitted with a hockey helmet instead of a football helmet as was used in this research, which has different material properties and characteristics.

The MPS results for forearm or elbow strikes to the head in the present study, on average (0.192), represent a 50% probability of concussion proposed by Zhang, Yang, & King (2004): 0.19 in the midbrain. The brain region studied and the material properties of the model in the region under examination play a role in the threshold values for risk of concussion (Zhang et al., 2004). Average MPS for impacts representing fall impacts in this research (0.4696) approach the threshold proposed by Patton et al. (2013) as the mean strain for concussion cases in their data set of head impacts in Australian football and rugby. These researchers separated MPS tolerance levels for concussion by brain region, which was not done in the current study. Patton et al.'s mean strain results for concussion ranged from 0.25 in the midbrain to 0.47 in gray matter. This suggests that impacts conducted on the monorail in this study mimicking falling to the ground result in magnitudes of brain trauma within the range of concussive impacts. The mean MPS for head to head impacts in the current study, 0.5956, is comparable to the mean strain reported by Takhounts et al. (2008) for head impacts among collegiate American football players, which was 0.5795. Interestingly, although these cases used by Takhounts et al. were reported to be the most severe of the football season, none resulted in a diagnosed brain injury. According to Galbraith et al. (1993), all three of the

mechanisms showed an average MPS above the threshold for reversible injury to brain tissue (0.1). Average MPS for all impacts representing the head to head and the fall impacts were also above an identified threshold for both functional deficit and structural failure (0.2 and 0.25 respectively) (Galbraith et al., 1993).

Peak VMS has been shown to be a good predictor of injury to brain tissue, although it has no physical interpretation except as an effective shear stress measure. It has been found to be a predictor of axonal injury in particular (Nishimoto et al., 1998). VMS was shown to be moderately positively correlated with linear acceleration for impacts representing falls to the ground ( $r = 0.42$ ). VMS was positively correlated with linear acceleration for impacts representing head to head collisions and when all three impact mechanisms were considered together ( $r = 0.858$  and  $0.852$  respectively). Prior research shows a moderate positive correlation ( $r = 0.52$ ) between linear acceleration and VMS for helmeted head impacts (Forero Rueda et al., 2011).

Consistent with observations for MPS, the low energy of the impacts conducted on the pendulum to represent forearm or elbow blows to the head may have played a role in the lack of a significant correlation for VMS. Head impacts at this energy level, which had an average linear acceleration of  $39.33g$  and a lower mass than the other two mechanisms, resulted in an average VMS of  $5805.9$  Pa. Based on thresholds proposed by Kleiven (2007) and Zhang et al. (2004), VMS at this magnitude represents less than 50% probability of sustaining a concussion:  $8.4$  kPa and  $7.8$  kPa, respectively. However, repetitive low energy impacts have been implicated in the development of neurological disorders and neurodegenerative diseases like chronic traumatic encephalopathy (McKee et al., 2013). This phenomenon has been observed

in boxers and some football players. Thus, the lack of a predictive ability of linear acceleration on stress and strain in the brain is an issue of concern. Helmets and impact sensors designed and certified according to linear acceleration alone as an injury metric is insufficient when protection against accumulating low energy impacts is needed. Impacts representing head to head collisions, which had an average VMS of 19,866.9 Pa, and those representing head impacts as a result of falling, for which average VMS was 14,475.4 Pa, represented similar levels of concussion risk. Further, the VMS results for these two mechanisms are in line with literature reporting a 50% concussion risk for a VMS level of 18 kPa (Willinger & Baumgartner, 2003), with the results for head to head hits being slightly above and falls being slightly below this threshold.

The third parameter examined in this study, strain rate, calculated as  $d\epsilon/dt$ , has been suggested as a tissue-level brain injury predictor by King et al. (2003). Past research has postulated that since the brain is composed of a viscoelastic biological tissue, its response to applied strain depends on the magnitude as well as the rate of such loading (Prange & Margulies, 2002; Brands et al., 2000). King et al. (2003) first presented strain rate as an injury metric on a macroscopic level. In the present analysis, strain rate was shown to have a moderate and positive correlation with linear acceleration of the head for head-to-head impacts, falls, and when all three mechanisms were examined as a whole ( $r = 0.424, 0.495, 0.585$  respectively). Compared to MPS and VMS, the strength of the correlation of strain rate with linear acceleration was notably lower. Again, like the findings for MPS and VMS, no correlation of linear acceleration with strain rate was found for impacts intended to represent arm or elbow strikes to the head.

The range of magnitude of strain rate obtained in this research for head to head, arm to head, and fall mechanisms of head impact (196.4, 95.7, 145.2  $s^{-1}$  respectively) were considerably above the 50% risk proposed by Kleiven of 48.5  $s^{-1}$  (2007). Interestingly, arm or elbow strikes to the head in this study were associated with a higher probability of concussive injury when quantified by strain rate than by MPS. The average strain rate for all three mechanisms were above the 50% risk for brain injury identified by King et al. (2003), which was identified to be 23 – 140  $s^{-1}$ .

A high number of correlation analyses were completed in this research, which statistically increases the probability that some of the correlational comparisons will be statistically significant by chance. When the data for all three impact mechanisms were combined in this study, there is a possibility that the higher and more significant correlation results occurred due to chance. Thus, the magnitude and the significance level of the correlations for all data combined should be taken conservatively.

## **5.2 Influence of impact location and mechanism on the relationship between linear acceleration and deformation metrics**

The two independent variables in this research, impact mechanism and location on the head, were varied to represent different conditions in which football players sustain impacts to the head. These variables were maximized in order to establish a wider range over which to examine the correlation of linear acceleration with the tissue deformation metrics.

An important observation consistent across all tissue deformation variables was the statistically significant high correlation between linear acceleration and deformation variables

for all head-to-head and fall impacts. The only exception was the insignificant correlation between linear acceleration and MPS for impacts that represented falls. However, the correlations of linear acceleration with each of MPS, VMS, and strain rate for the impacts that were delivered to the Hybrid III headform by the pendulum system were not significant for any condition. These impacts were meant to mimic low-energy impacts to the head by the forearm or elbow such as a forearm shiver play in football. Due to the low inbound mass and low velocity, the pendulum frame pushed the helmeted headform out of the way during these impacts, resulting in rotation of the head. Thus, impacts occurring via this mechanism were rotationally dominant in nature. In contrast, impacts intended to represent falls and head to head collisions had a much higher energy and the energy of the impact was linearly directed through the centre of gravity of the headform. These were linear-dominant events. It was expected that the results of this study show significant correlations between linear acceleration and the deformation variables for the two linear-dominant impact mechanisms. For head impacts with low inbound energy rotational acceleration would likely show greater association with stresses and strains in the brain tissue.

Multiple input parameters were encompassed by the variable of impact mechanism in this study. Velocity, mass, and compliance were distinct for each of the three mechanisms. Differences among these input parameters would help to explain some of the variability between correlations the three impact mechanisms examined.

Although trends between the impact mechanisms can be identified, the purpose of this research was not to compare results at each impact location across the three mechanisms. The

goal was not to attempt to reconstruct specific, real-world events but to obtain a realistic range over which the relationship between two dependent variables could be examined.

The second independent variable, impact location on the head, also had an important influence on the association between the kinematic parameter of linear acceleration and metrics of deformation of the underlying brain tissue. Location of impact on the head affecting the association of metrics of brain deformation to linear acceleration depending on impact position is consistent with the literature (Forero Rueda et al., 2011). The nine impact sites in this study were selected based on prior research showing an increased risk of injury for particular location and angle combinations on a Hybrid III headform (Walsh, Rousseau, & Hoshizaki, 2011). Some were centric in nature, which means that the vector of the impact was directed through the head's centre of gravity, while others were non-centric impacts. The centric impact locations were front boss CG, side CG, rear boss CG, and rear CG. Non-centric impact locations comprised the remainder of the nine sites: front positive elevation 15, front boss PA, rear boss NA, rear NA, and front faceguard. The average linear acceleration, MPS, and VMS was higher for the centric impact sites, all three of the impact mechanisms considered, than for the non-centric sites. Strain rate was the only dependent variable that was higher on average for the non-centric sites than for the centric.

In terms of the strength of correlation between the three brain deformation variables with linear acceleration, the correlation with all of the tissue deformation metrics, MPS, VMS, and strain rate, was higher for the centric sites than for the non-centric sites, on average. This finding is consistent with results reported by Post et al. (2012) that show that correlations between linear acceleration of the head and brain deformation exist for centric impact

locations but not for non-centric impacts. The impact protocol used by these authors, as in the present study, used the UOTP-9 impact protocol to a Hybrid III headform outfitted with a conventional football helmet.

The level of association between peak linear acceleration and the brain deformation values essentially measures the degree to which linear acceleration as a metric of impact severity is consistent with the amount of distortion that is occurring to the brain tissue upon impact, which has been shown to be most predictive of injury. Universal peaks of brain tissue deformation in the cerebrum were measured and analyzed in this study. If peak values of tissue deformation in particular locations were considered instead of an overall global peak, it is likely that the peaks would be found in both the area of the brain that was impacted as well as the *contrecoup* region from the region of impact.

### **5.3 Significance**

The strength of the correlations varied substantially across impact mechanisms and locations on the head. This suggests that parameters of an impact such as velocity, impact site, and compliance influence the relationships. For particular impact mechanisms and locations on the head, peak linear acceleration is effective at estimating and representing risk of injury to the brain tissue. As this study examined the sport of football specifically, it was concluded that peak resultant linear acceleration is a moderately effective correlate of brain tissue deformation metrics for the mechanisms by which football players get hit to the head. Overall, linear acceleration was most effective for head to head collisions, followed by falls to the ground, and was least effective for forearm or elbow to head impacts. However, it has been

reported by epidemiological research that football players are hit in the head according to the upper extremity to head mechanism frequently (Withnall et al., 2005). The effectiveness of linear acceleration as a representation of tissue deformation specific to sports other than football would likely be different than the findings of this study for football. Players of other sports typically suffer head impacts according to different mechanisms and locations than do football players.

Impacts to a Hybrid III headform delivered by the pendulum system in this study, meant to mimic strikes to the head by another player's elbow or forearm, was the only impact mechanism for which linear acceleration consistently showed no significant correlation with any of the brain deformation metrics. Thus, peak resultant linear acceleration seems to be ill suited to serving as a predictor of brain tissue response to an impact for low-energy impacts in particular. The results of this research support using metrics of deformation of brain tissue for designing and evaluating the performance of American football helmets in order to protect against injury. Since significant correlations were observed between linear acceleration and measures of trauma to brain tissue for head to head collisions and falls (except in the case of MPS), continuing to use linear acceleration to design and certify head protection products may be appropriate when considering higher-energy, more linear-dominant impacts. However, in order for head protective headgear to effectively protect against head impacts across the full spectrum of severity, more direct metrics of tissue deformation should be considered.

An additional factor that affected the correlation between kinematic variables and stresses and strains is the brain tissue type. Distinct tolerance values for loading and different geometry as well as material characteristics both influence brain tissue response (Prange et al.,

2002). Separating the deformation results by different tissue types in the brain would be an interesting future extension of this work.

The correlation between rotational acceleration of the head and the three brain tissue deformation variables was not examined in this research because rotational acceleration has only recently been recognized in the scientific community as an important metric for head injury. In turn, manufacturers of protective equipment for the head currently continue to rely largely on linear acceleration for certification testing and development of such products. As a continuation of this work, future research should investigate the correlation between rotational acceleration and brain tissue deformation variables, however. This would provide information about whether rotational acceleration would be a better or sufficient metric to use to evaluate the effectiveness of protective technology to protect against trauma that football players are actually sustaining during the sport.

This research provided a systematic examination of the degree of correlation that linear acceleration of the head showed with three deformation metrics shown to be associated with injury, for 27 unique conditions. The ranges of the input parameters of mass, velocity, compliance, and location, were maximized among the three impact mechanisms. This research is also unique in that all of the impact conditions were representative of ways in which American football players most frequently get injured. As football is the sport responsible for the highest concussion incidence, this study offers insight into the effectiveness of linear acceleration as an estimate for trauma to the brain unique to head impacts sustained in this sport.

## CHAPTER 6

### Conclusions

#### 6.1 Research Hypotheses

The hypotheses that the strength of the correlation of peak resultant linear acceleration with MPS, VMS, and strain rate would be low were, overall, shown to be incorrect. When all three impact mechanisms of impact and all nine locations of impact were considered, the strength of each correlation was characterized by a Pearson correlation coefficient greater than  $r = 0.5$ .

H1: LA and MPS will have a low positive correlation ( $r < 0.5$ ) for all impact mechanisms and locations.

i. Rejected

H2: LA and VMS will have a low positive correlation ( $r < 0.5$ ) for all impact mechanisms and locations.

i. Rejected

H3: LA and Strain Rate will have a low positive correlation ( $r < 0.5$ ) for all impact mechanisms and locations.

i. Rejected

## 6.2 Summary

Linear acceleration remains widely used for design and testing certification of helmets and other head protection technologies. The purpose of this research was to investigate the degree of association between this widely-used kinematic variable, peak resultant linear acceleration, and three metrics of trauma to brain tissue. The rationale for this work was to investigate the degree of association between peak resultant linear acceleration and metrics of brain tissue deformation, in light of the advent of protective technology such as head impact sensors and counters. Many of such products base estimation of injury risk on linear acceleration. The results of this research showed that linear acceleration was moderately correlated with all of MPS, VMS, and strain rate for at least one of the impact mechanisms. The degree of correlation increased when all three impact mechanisms were examined together as a whole. In terms of impact location on the head, centric impacts showed higher average values than non-centric impacts for linear acceleration and all of the brain deformation metrics examined except strain rate. This observation again suggests an association between linear acceleration and measures of stress and strain to the brain tissue itself.

These findings suggest other characteristics of an impact, such as the inbound energy, whether the vector of impact was centric or non-centric, and the degree of energy transfer that occurs through the head upon impact, likely play a role in the resulting degree of association between linear acceleration and tissue stress or strain. As a result, linear acceleration as a metric of injury risk may be appropriate for testing protective headgear for football. However, its effectiveness as a proxy for brain tissue deformation metrics is limited to head impacts of a particular nature. According to the results, thorough head protection in the

game, and particularly protection against low-energy impacts, would require the consideration of other measures such as rotational acceleration, strain, and stress.

## References

- American Association of Neurological Surgeons. (2011). Concussion. Retrieved from: <http://www.aans.org/en/Patient%20Information/Conditions%20and%20Treatments/Concussion.aspx>.
- American College of Surgeons: Committee on Trauma. (1998). Management of Head Injury.
- Anderson RWG, Brown CJ, Blumbergs PC, Scott G, Finney JW, Jones NR, McLean AJ. (1999). Mechanisms of axonal injury: an experimental and numerical study of a sheep model of head impact. *Proceedings of the International Research Conference on the Biomechanics of Injury (IRCOBI)*, Stiges, Spain.
- Bain AC, Meaney DF. (2000). Tissue-level thresholds for axonal damage in an experimental model of central nervous system white matter injury. *Journal of Biomechanical Engineering*. 122, 615-622.
- Bandak, F.A., and Eppinger, R.H. (1994). A three-dimensional FE analysis of the human brain under combined rotational and translational accelerations. *Proceedings 38<sup>th</sup> Stapp Car Crash Conference*, 145-163.
- Baugh CM, Stamm JM, Riley DO, et al. (2012). Chronic traumatic encephalopathy: neurodegeneration following repetitive concussive and subconcussive brain trauma. *Brain Imaging and Behaviour*. 6, 244-254.
- Brands DW, Bovendeerd PH, Peters GW, Wismans JS. (2000). The large shear strain dynamic behavior of in-vitro porcine brain tissue and a silicone gel model material. *Stapp Car Crash Journal*. 44, 249-260.
- Cantu RC & Mueller FO. (2003). Brain injury-related fatalities in American football, 1956-1999. *Neurosurgery*. 52(4), 846-853.
- Cater HL, Sundstrom LE, Morisson III, B. (2006). Temporal development of hippocampal cell death is dependent on tissue strain but not strain rate. *Journal of Biomechanics*. 39, 2810-2818.
- Centers for Disease Control and Prevention: Sport-related recurrent brain injuries. (1997). *MMWR Morb Mortal Wkly Rep*. 46:224-227.
- Cearnal, L. (2012). Chronic Traumatic Encephalopathy: Emergency physicians fielding more questions in the absence of evidence. *Annals of Emergency Medicine*. 60(4),A17-A21.
- Crisco JJ, Fiore R, Beckwith JG, Chu JJ, Brolinson PG, Duma S, McAllister TW, Duhaime A-C, & Greenwald RM (2010). Frequency and location of head impact exposures in individual collegiate football players. *Journal of Athletic Training*, 45(6), 549-559.
- Crisco JJ, Wilcox BJ, Beckwith JG, Chu JJ, Duhaime A-C, Rowson S, Duma SM, Maerlender AC, McAllister TW, Greenwald RM. (2011). Head impact exposure in collegiate football players. *Journal of Biomechanics*. 44; 2673-2678.
- Covassin T, Swanik CB, Sachs ML. (2003). Epidemiological considerations of concussions among intercollegiate athletes. *Applied Neuropsychology*. 10(1); 12-22.
- Delaney JS, Lacroix VJ, Leclerc S, Johnston KM. (2000). Concussions during the 1997 Canadian Football League Season. *Clinical Journal of Sport Medicine*. 10(1); 9-14.
- Delaney JS, Lacroix VJ, Leclerc S, Johnston KM. (2002). Concussions among university football and soccer players. *Clinical Journal of Sport Medicine*. 12 (6); 331-338.

- Deng YC. (1989). Anthropomorphic dummy neck modeling and injury reconstructions. *Accident Analysis & Prevention*. 21(1); 85-100.
- Doorly MC, Gilchrist MD. (2006). The use of accident reconstruction for the analysis of traumatic brain injury due to head impacts arising from falls. *Computer Methods in Biomechanics and Biomedical Engineering*. 9(6) ; 371-377.
- Forero Rueda MA, Cui L, Gilchrist MD. (2011). Finite element modelling of equestrian helmet impacts exposes the need to address rotational kinematics in future helmet designs. *Computer Methods in Biomechanics and Biomedical Engineering*. 14(12); 1021-1031.
- Galbraith J, Thibault L, Matteson D. (1993). Mechanical and electrical responses of the squid giant axon to simple elongation. *Journal of Biomechanical Engineering*. 115; 13-22.
- Gennarelli, T.A.; Ommaya A.K.; Thibault, L.E. (1971) Comparison of translational and rotational head motions in experimental cerebral concussion. Proc. 15<sup>th</sup> Stapp Car Crash Conference, SAE P-39: 797-803.
- Gennarelli, T.A.; Thibault, L.E.; Ommaya, A.K. (1972) Pathophysiologic responses to rotational and Linear accelerations of the head. Proc 16<sup>th</sup> Stapp Car Crash Conference, SAE Paper No. 720970.
- Gennarelli, T.A.; Adams, J.H.; Graham, D.I. (1981) Acceleration induced head injury in the monkey I: The model, its mechanistic and physiological correlates. *Acta Neuropathol. Suppl.*, 7:23-25.
- Gennarelli, T.A.; Thibault, L.E.; Adams, J.H.; Graham, D.I.; Thompson, C.J.; Marcincin, R.P. (1982a) Diffuse axonal injury and traumatic coma in the primate. *Ann Neurol.*,12:564-574.
- Gennarelli, T.A.; Thibault, L.E. (1982b) Biomechanics of acute subdural hematoma. *J. Trauma.*, 22: 680-686.
- Gilchrist MD & O'Donoghue D. (2000). Simulation of the development of frontal head impact injury. *Computational Mechanics*. 26(3), 229-235.
- Gilchrist MD, O'Donoghue D, Horgan TJ. (2001). A two-dimensional analysis of the biomechanics of frontal and occipital head impact injuries. *International Journal of Crashworthiness*. 6(2), 253-262.
- Goldsmith W. (1981). Current controversies in the stipulation of head injury criteria. *Journal of Biomechanics*. 14(12), 883-884.
- Gurdjian ES & Lissner HR. (1941). Mechanism of head injury as studied by the cathode ray oscilloscope: Preliminary report. *Journal of Neurosurgery*.
- Gurdjian ES, Webster JE, Lissner HR. (1955). Observations on the mechanism of brain concussion, contusion, and laceration, *Surg Gynecol Obstet*. 101: 680-690.
- Gurdjian ES, Lissner HR, Latimer FR, Haddad BF, Webster JE. (1953). Quantitative determination of acceleration and intracranial pressure in experimental head injury: Preliminary report. *Neurology*. 3(6), 417-423.
- Guskiewicz KM, Weaver NL, Padua DA, Garrett WE. (2000). Epidemiology of concussion in collegiate and high school football players. *The American Journal of Sports Medicine*. 28(5); 643-650.
- Guskiewicz KM, Marshall SW, Bailes J, McCrea M, Cantu RC, Randolph C, Jordan BD. (2005). Association between recurrent concussion and late-life cognitive impairment in retired professional football players.

- Hardy, W.N., Foster, C.D., Mason, M.J., Yang, K.H., King, A.I., and Tashman, S. (2001). Investigation of head injury mechanisms using neutral density technology and high-speed biplanar x-ray. *Stapp Car Crash Journal*, The Stapp Association, Ann Arbor, Michigan.
- Harmon KG, Drezner J, Gammons M, Guskiewicz K, Halstead M, Herring S, Kutcher J, Pana A, Putukian M, Roberts W. (2013). American Medical Society for Sports Medicine Position Statement: Concussion in Sport. *Clinical Journal of Sports Medicine*. 23, 1-18.
- Holbourn AHS. (1943). The mechanics of head injuries. *Lancet*. 2, 438-441.
- Horgan, T.J. (2005). A finite element model of the human head for use in the study of pedestrian accidents. PhD Thesis, University College Dublin, Dublin Ireland.
- Horgan, T.J. and Gilchrist, M.D. (2003). The creation of three-dimensional finite element models for simulating head impact biomechanics. *IJCrash*, 8 (4), 353-366.
- Horgan, T.J., and Gilchrist, M.D. (2004). Influence of FE model variability in predicting brain motion and intracranial pressure changes in head impact simulations. *IJCrash*, 9 (4), 401-418.
- Hu H, et al. (1998). Modeling human brain movability effect on brain response during impact. *ASME Mechanical Engineering Congress and Exposition*. AMD 230, ASME, 267-280.
- Kang HS, Willinger R, Diaw BM, Chinn B. (1997). Validation of a 3D anatomic human head model and replication of head impact in motorcycle accident by finite element modeling. *Proceedings of the 41st Stapp Car Crash Conference, November 13-14, 1997, Orlando Florida, USA*.
- King AI, Ruan JS, Zhou C, Hardy WN, Khalil TB. (1995). Recent advances in biomechanics of brain injury research: A review. *Journal of Neurotrauma*. 12(4), 651-657.
- King AI, Yang KH, Zhang L, Hardy W. (2003). Is head injury caused by linear or angular acceleration? *Proceedings of IRCOBI*. Lisbon, Portugal.
- Kleiven, S., and Von Holst, H. (2002). Consequences of size following trauma to the human head. *Journal of Biomechanics*, 35, 135-160.
- Kleiven S. (2007). Predictors for traumatic brain injuries evaluated through accident reconstructions. *Stapp Car Crash Journal*. 51, 81-114.
- Langburt W, Cohen B, Akhthar N, O'Neill K, Lee JC. (2001). Incidence of concussion in high school football players of Ohio and Pennsylvania. *Journal of Child Neurology*. 16(2), 83-85.
- Leibson CL, Brown AW, Hall Long K, Ransom JE, Mandrekar J, Osler TM, et al. (2012). Medical Care Costs Associated with Traumatic Brain Injury over the Full Spectrum of Disease: A Controlled Population-Based Study. *Journal of Neurotrauma*. 10.1089/neu.2010.1713
- Levy ML, Ozgur BM, Berry C, Aryan HE, Apuzzo MLJ. (2004). Analysis and evolution of head injury in football. *Neurosurgery*. 55(3), 649-655.
- Marar M, McIlvain NM, Fields SK, Comstock RD. (2012). Epidemiology of concussions among United States high school athletes in 20 sports. *American Journal of Sports Medicine*. 40(4), 747-755.
- Max W, MacKenzie EJ, Rice DP. (1991). Head Injuries: Costs and Consequences. *Journal of Head Trauma and Rehabilitation*. 2:76-91.

- McCrea M, Hammeke T, Olsen G, Leo P, Guskiewicz K. Unreported concussion in high school football players: Implications for prevention. *Clinical Journal of Sport Medicine*. 14(1), 13-17.
- McCrory P, Meeuwisse WH, Kutcher JS, Jordan BD, Gardner A. (2013). What is the evidence for chronic concussion-related changes in retired athletes: behavioural, pathological and clinical outcomes? *British Journal of Sports Medicine*. 47; 327-330.
- Mendis, K., Stalnaker, R., and Advani, S. (1995). A constitutive relationship for large deformation finite element modeling of brain tissue. *Journal of Biomechanical Engineering*, 117(4), 279-285.
- McKee AC, Stein TD, Nowinski CJ, et al. (2013). The spectrum of disease in chronic traumatic encephalopathy. *Brain*. 136,43-64.
- Miller, R., Margulies, S., Leoni, M., Nonaka, M., Chen, Z., Smith, D., and Meaney, D. (1998). Finite element modeling approaches for predicting injury in an experimental model of severe diffuse axonal injury. In Proceedings of the 42<sup>nd</sup> Stapp Car Crash Conference, SAE paper No. 983154.
- Morrison III. B, Cater HL, Wang CB, Thomas FC, Hung CT, Ateshian GA, Sundstrom LE. (2003). A tissue level tolerance criteria for living brain developed with an in vitro model of traumatic mechanical loading. *Stapp Car Crash Journal*. 47, 93-105.
- Nahum, A.M., Smith, R., and Ward, C.C. (1977). Intracranial pressure dynamics during head impact. Proceedings 21<sup>st</sup> Stapp Car Crash Conference. SAE paper No. 770922.
- Neselius S, Brisby H, Theodorsson A, Blennow K, Zetterberg H, et al. (2012) CSF-Biomarkers in Olympic Boxing: Diagnosis and Effects of Repetitive Head Trauma. *PLoS ONE* 7(4): e33606. doi:10.1371/journal.pone.0033606
- Nolan S. (2005). Traumatic brain injury: a review. *Critical Care Nursing Quarterly*. 28(2), 188-194.
- Oeur A. et al. (2013). Examination of headform dynamic response for concussive injuries and traumatic brain injuries. *Helmet Performance & Design Conference February 2013, London UK*.
- Ommaya AK, Goldsmith W, & Thibault L. (2002). Biomechanics and neuropathology of adult and paediatric head injury. *British Journal of Neurosurgery*. 4(1), 13-31.
- Padagaonkar AJ, Krieger KW, and King AI (1975) Measurement of angular acceleration of a rigid body using linear accelerometers. *J Appl Mech* 42:552-556.
- Patton DA, McIntosh AS, Kleiven S. (2013). The biomechanical determinants of concussion: Finite element simulations to investigate brain tissue deformations during sporting impacts to the unprotected head. *Journal of Applied Biomechanics*. 29; 721-730.
- Pellman EJ, Powell JW, Viano DC, Casson IR, Tucker AM, Feuer H, Lovell M, Waeckerle JF, Robertson DW. (2004). Concussion in professional football: Epidemiological features of game injuries and review of the literature: Part 3. *Neurosurgery*. 54(1);81-96.
- Pellman EJ, Viano DC, Tucker AM, & Casson IR (2003). Concussion in professional football: Location and direction of helmet impacts – Part 2. *Neurosurgery*, 53(6), 1328-1341.
- Pellman EJ, Viano DC, Whitnall C et al (2006) Concussion in professional football: Helmet testing to assess impact performance – Part 11. Neurosurgery 58:78-95.*

- Pellman EJ. (2003). Background on the National Football League's research on concussion in professional football. *Neurosurgery*. 53:797–798.
- Post A, Oeur A, Hoshizaki TB, Gilchrist MD. (2011). Examination of the relationship between peak linear and angular accelerations to brain deformation metrics in hockey helmet impacts. *Computer Methods in Biomechanics and Biomedical Engineering*.
- Post A, Walsh ES, Hoshizaki TB, Gilchrist MD. (2012)<sup>a</sup>. Analysis of loading curve characteristics on the production of brain deformation metrics. *Journal of Sports Engineering and Technology*. 226(3/4), 200-207.
- Post A, Oeur A, Hoshizaki TB, Gilchrist MD. (2012)<sup>b</sup>. The influence of centric and non-centric impacts to American football helmets on the correlation between commonly used metrics in brain injury research. *Proceedings of the International Research Conference on the Biomechanics of Injury (IRCOBI)*, Dublin, Ireland.
- Post A & Hoshizaki TB. (2012)<sup>c</sup>. Mechanisms of brain impact injuries and their prediction: A review. *Trauma*. 4(4), 327-349.
- Post A et al. (2013). On the importance of using a centric/non-centric protocol for the evaluation of hockey helmet performance. Submitted.
- Prange MT, Margulies SS. (2002). Regional, directional, and age-dependent properties of the brain undergoing large deformation. *Journal of Biomechanical Engineering*. 124, 244-252.
- Ruan JS, Khalil T, King AI. (1993). Finite element modeling of direct head impact. *Proceedings of the 37<sup>th</sup> Stapp Car Crash Conference*, pp. 69-81. Society of Automotive Engineers, Warrendale PA.
- Schnebel B, Gwin JT, Anderson S, Gatlin R. (2007). In vivo study of head impacts in football: A comparison of national collegiate athletic association division I versus high school impacts. *Neurosurgery*. 60(3), 490-496.
- Seemann MR, Muzzy WH, Lustick LS. (1986). Comparison of human and Hybrid III head and neck dynamic response. *Stapp Car Crash Journal*. 30th Proceedings, 291–311.
- Shreiber DI, Bain AC, Meaney DF. (1997). In vivo thresholds for mechanical injury to the blood-brain barrier. *Stapp Car Crash Journal*. 41, 277-291.
- Shugar, T. and Katona, M. (1975). Development of a finite element head injury model. ASCE, *Journal of Engineering mechanics*, EM3 (E101/173), 223-239.
- Society of Automotive Engineers International (2007) Instrumentation for Impact Test – Part 1 – Electronic Instrumentation. Surface Vehicle Recommended Practice, J211-1*
- Takhounts EG, Ridella SA, Hasija V, et al. (2008). Investigation of traumatic brain injuries using the next generation of simulated injury monitor (SIMon) finite element head model. *Stapp Car Crash J*. 52:1–31
- Thibault, L.E.; Gennarelli, T.A. (1985) Biomechanics of diffuse brain injuries. Proc. 29<sup>th</sup> Stapp Car Crash Conference, SAE Paper No. 856022.
- Thunna DJ, Branche CM, Sniezek JE. (1998). The epidemiology of sports-related traumatic brain injuries in the United States: Recent developments. *Journal of Head Trauma Rehabilitation*. 13(2); 1-8.

- Trosseille, X., Tarrière, C., Lavaste, F., Guillon, F., and Domont, A. (1992). Development of a F.E.M. of the human head according to a specific test protocol. Proceedings of the 36<sup>th</sup> Stapp Car Crash Conference, Seattle, Washington, USA, SAE 922527.
- Viano DC, Lau IV, Asbury C, King AI, Begeman P. (1989). Biomechanics of the human chest, abdomen, and pelvis in lateral impact. *Accident Analysis and Prevention*. 21(6), 553-574.
- Ward, C. and Thompson, R.B. (1975). The development of a detailed finite element brain model. Proceedings of the 19<sup>th</sup> Stapp Car Crash Conference, San Diego, California, USA, SAE 751163.
- Willinger R & Baumgartner D. (2003). Human head tolerance limits to specific injury mechanisms. *International Journal of Crashworthiness*. 8(6), 605 — 617.
- Willinger R, Taleb L, Kopp CM. (1995). Modal and temporal analysis of head mathematical models. *Journal of Neurotrauma*. 12(4), 743-754.
- Withnall C, Shewchenko N, Gittens R, Dvorak J. (2005). Biomechanical investigation of head impacts in football. *British Journal of Sports Medicine*. 39(Suppl 1): i49-i57.
- Zhang L, Yang KH, King AI. (2004). A proposed injury threshold for mild traumatic brain injury. *J Biomech Eng*;126:226-236.
- Zhang L, Yang KH, King AI. (2001). Comparison of brain responses between frontal and lateral impacts by finite element modeling. *Journal of Neurotrauma*. 18(1), 21-31.
- Zhang L. (2001). Computational biomechanics of traumatic brain injury: An investigation of head impact response and American football head injury. (Doctor of Philosophy thesis). Wayne State University, Detroit, Michigan.
- Zhou, C., Khalil, T., King, A. (1994). Shear Stress Distribution in the Porcine Brain due to Rotational Impact. SAE Technical Papers. doi:10.4271/942214.
- Zhou C, Khalil TB, Dragovic LJ. (1996). Head injury assessment of a real world crash by finite element modeling. *Proceedings of the AGARD Conference*. New Mexico, USA, November 1996.

**Appendix A**  
**Impact Locations: University of Ottawa Test Protocol-9**

Front



Front positive elevation 15°



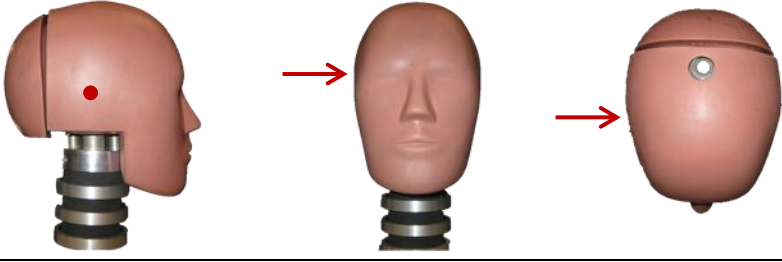
Front Boss Centre Gravity



Front Boss Positive Azimuth



Side Centre Gravity



Rear Boss Negative Azimuth



Rear Boss Center Gravity



Rear Negative Azimuth



Rear Centre of Gravity



Front Face Guard

